Multi-functional hybrid energy system for zero-energy residential buildings: Integrating hydrogen production and renewable energy solutions

International Journal of Hydrogen Energy 102 (2025) 647–672

Contents lists available at ScienceDirect

International Journal of Hydrogen Energy

journal homepage: www.elsevier.com/locate/he

Multi-functional hybrid energy system for zero-energy residential buildings: Integrating hydrogen production and renewable energy solutions

Saleh Mobayen [a,1], Ehsanolah Assareh [b,1], Nima Izadyar [b,c,1,*], Elmira Jamei [b,c], Mehrdad Ahmadinejad [d], Amir Ghasemi [e], Saurabh Agarwal [f,1], Wooguil Pak [f,**]

[a] Graduate School of Intelligent Data Science, National Yunlin University of Science and Technology, Douliu, Yunlin, 640301, Taiwan
[b] Built Environment and Engineering Program, College of Sport, Health and Engineering (CoSHE), Victoria University, Melbourne, VIC 3011, Australia
[c] Institute for Sustainable Industries and Liveable Cities, Victoria University, Melbourne, VIC, 3011, Australia
[d] Department of Mechanical Engineering, University of Vermont, Burlington, VT, USA
[e] Department of Civil Engineering, School of Engineering, Monash University, Clayton Campus, Melbourne, VIC, 3800, Australia
[f] Department of Information and Communication Engineering, Yeungnam University, Gyeongsan 38541, South Korea

ARTICLE INFO

Keywords:
Artificial neural network optimization
Brayton cycle
Exergy efficiency
Multi-generation system
Proton exchange membrane electrolyzer
Wind power

ABSTRACT

The increasing global residential energy demand causes carbon emissions and ecological impacts, necessitating cleaner, efficient solutions. This study presents an innovative hybrid energy system integrating wind power and gas turbines for a four-story, 16-unit residential building. The system generates electricity, heating, cooling, and hydrogen using a Proton Exchange Membrane electrolyzer and a compression chiller. Integrating the electrolyzer enables hydrogen production and demonstrates hydrogen's potential as a versatile, clean energy carrier for systems, contributing to advancements in hydrogen utilization. Simulations with Engineering Equation Solver software, coupled with neural network-based multi-objective optimization, fine-tuned parameters such as gas turbine efficiency, wind turbine count, and gas turbine inlet temperature to enhance exergy efficiency and reduce operational costs. The optimized system achieves an energy efficiency of 33.69% and an exergy efficiency of 36.95% and operates at $446.04 per hour, demonstrating economic viability. It produces 51,061 MWh annually, exceeding the building's energy demands and allowing surplus energy use elsewhere. BEopt simulations confirm the system meets residential needs by providing 2.52 GWh of electricity, 3.36 GWh of heating, and 5.11 GWh of cooling annually. This system also generates 10 kg of hydrogen per hour and achieves a CO_2 reduction of 10,416 tons/year. The wind farm (25 turbines) provides most of the energy at 396.7 dollars per hour, while the gas turbine operates at 80% efficiency. By addressing the challenges of intermittent renewable energy in residential Zero-Energy Buildings, this research offers a scalable and environmentally friendly solution, contributing to sustainable urban living and advancing hydrogen energy applications.

Nomenclature

Abbreviations	Description	Symbol	Description
ANN	*Artificial Neural Network*	C_P	*Specific heat Coefficient at constant pressure [kJ/kg.K]*
BEopt	*Building Energy Optimization*	$\dot{E}x$	*Exergy [kW]*
CC	*Combustion chamber*	h	*Specific enthalpy [kj/kg]*
CHP	*Combined Heat and Power*	$\dot{m}$	*Mass flow rate [kg/s]*
CRF	*Capital Recover Factor*	P	*Pressure [kPa]*
CO_2	*Carbon Dioxide*	T	*Temperature [°C]*
DC	*Direct Current*	U	*Overall heat transfer coefficient [kW/m^{2}K]*
GAs	*Genetic Algorithms*	$\dot{W}$	*Power [kW]*

(continued on next column)
(continued)
(continued on next page)

* Corresponding author. Built Environment and Engineering Program, College of Sport, Health and Engineering (CoSHE), Victoria University, VIC 3011, Melbourne, Australia.
** Corresponding author.
E-mail addresses: nima.izadyar@vu.edu.au (N. Izadyar), wooguilpak@yu.ac.kr (W. Pak).
[1] These authors contributed equally to this article as the first author.

https://doi.org/10.1016/j.ijhydene.2025.01.061
Received 17 November 2024; Received in revised form 25 December 2024; Accepted 6 January 2025
Available online 11 January 2025

(*continued*)

GT	*Gas turbine*	*Z*	*Investment cost [$]*
LCC	*Life Cycle Cost*	$\dot{Z}$	*Cost rate [$/h]*
LED	*Light Emitting Diode*	**Subscripts**	**Description**
MOO	*Multi-Objective Optimization*	*ch*	*Chemical*
PCM	*Phase Change Material*	*cv*	*control volume*
PEM	*Proton Exchange Membrane*	*in*	*Inlet*
PEME	*PEM Electrolyzer*	*ex*	*exergy*
PV	*Photovoltaic*	*out*	*outlet*
SD	*Standard Deviation*	*ph*	*physical*
WT	*Wind turbine*	*Q*	*Cooling capacity*
ZEB	*Zero Energy Building*	*v*	*vapor*
Greek symbol	**Description**	*in*	*Inlet*
η	*Efficiency [%]*		
φ	*Maintenance factor*		
ρ	*Air density [kg/m^3]*		

1. Introduction

Wind energy, harnessed from ancient windmills to modern turbines, is a sustainable and abundant clean energy source [1,2]. Although wind power is a promising substitute for fossil fuels by contributing to lower CO_2 emissions and addressing rising energy demands [3,4], its intermittent nature limits its standalone application, and its potential may be constrained by climate change's impact on wind resources [5]. As residential energy demands grow rapidly [6], improving wind energy harvesting is becoming increasingly critical. Zero Energy Buildings (ZEBs), which produce as much energy as they consume and emit no Carbon Dioxide (CO_2) [7,8], offer a pathway to meeting these demands sustainably. However, a key challenge in achieving residential ZEBs lies in the variability of renewable sources and the associated need for efficient energy storage systems [9,10]. This difficulty is compounded by budget constraints for batteries and dependence on fossil fuels in extreme climates, where heating and cooling demands are higher [11]. In this context, hybrid energy systems, integrating wind energy with complementary technologies, provide a viable solution to ensure continuous power while reducing environmental impact [12]. Therefore, research into designing optimal ZEBs that integrate energy-efficient, multi-generation renewable systems is essential to achieve ZEB and reduce reliance on fossil fuels [13,14].

The literature shows that although progress is being made in utilizing hybrid renewable energy sources for domestic purposes, residential buildings still rely on fossil fuels and grids as backups, undermining the goal of achieving net-zero emissions [15]. It caused the number of residential ZEBs to remain low, even in OECD countries [16,17]. To overcome this challenge, it is crucial to identify reliable, practical, and low-emission alternatives that can serve as reliable backup systems, generating sufficient energy while reducing CO_2 emissions [18]. Gas turbines are among these reliable sources, operating on cleaner fuels like hydrogen, methane, and natural gas, emitting less CO_2 than conventional fossil fuels [19]. Hydrogen, a clean energy carrier, is compatible with multiple energy applications and provides an opportunity to enhance energy security, reduce emissions, and support the transition to sustainable energy systems globally [20–23]. The flexibility of gas turbines in fuel options [24], combined with the ability to integrate with renewable systems and utilize waste heat through Combined Heat and Power (CHP) applications, makes gas turbines an efficient and sustainable choice for ensuring consistent energy supply in residential ZEBs [25,26].

Gas turbines can generate substantial amounts of energy, meeting large energy demands. The Brayton cycle is used in gas turbines to maintain steady energy output when renewable sources are unavailable, ensuring continuous power [27]. This combination of renewable energy and gas turbines running on the Brayton cycle enables hybrid systems to meet fluctuating residential demands while minimizing environmental impact through reduced CO_2 emissions [28,29]. Integrating Proton Exchange Membrane (PEM) electrolyzers enhances hybrid systems by producing hydrogen, which can be stored and later consumed in gas turbines, emitting no pollutants when consumed, thereby increasing the system's flexibility and reliability by ensuring a consistent energy supply even when renewable sources are intermittent [30–32]. Hydrogen's role extends beyond energy storage, as it enables clean energy generation through thermochemical and electrochemical (e.g., PEM), aligning with international goals to develop sustainable hydrogen energy ecosystems [33]. By harnessing gas turbines and hydrogen production, hybrid systems offer a practical solution for achieving ZEBs in extreme climates, where a stable and low-emission energy source is essential.

To maximize hybrid systems' efficiency and minimize environmental impacts, it's critical to balance energy efficiency, cost, and environmental impact through optimization techniques [34]. This is even more important when applying hybrid systems in residential ZEBs due to fluctuating energy demands, affordability, and potential large-scale environmental impact [35]. Literature shows Artificial Neural Networks (ANNs) and Genetic Algorithms (GAs), as advanced machine learning techniques, can effectively improve the performance of hybrid systems by optimizing parameters such as fuel consumption, energy storage, and emissions [36–38]. These tools enable systems to adapt dynamically to changing energy demands and renewable availability, ensuring economic viability and environmental sustainability, making them suitable for widespread application in residential ZEBs [39,40].

This article introduces an innovative hybrid energy system that combines wind power with gas turbines enhanced by multi-objective optimization. By integrating PEM electrolyzers, the system advances hydrogen energy utilization and achieves high exergy efficiency, cost-effectiveness, and significant CO_2 reduction. These innovations set a new benchmark in achieving environmental sustainability and continuous energy supply for residential ZEBs, addressing gaps in existing systems with intermittent renewable sources. By offering a scalable solution that advances hydrogen energy utilization and aligns with global sustainable development goals, this hybrid system represents a meaningful contribution to hydrogen energy research. The paper proceeds: Section 2 describes the system configuration; Section 3 covers ANN-based modeling and optimization; Section 4 presents the governing equations; Section 5 discusses results and validation; Section 6 discusses limitations and future prospects; and Section 7 provides the study's conclusion.

2. System configuration and functionality

Fig. 1 illustrates the proposed system's schematic, which primarily harnesses wind energy from a wind farm, supported by a gas turbine, and incorporates a PEM electrolyzer and compression chiller. This design strategically integrates wind turbines with a PEM electrolyzer and gas turbine operating on the Brayton cycle, enabling the system to maximize energy capture while providing continuous power through hydrogen storage. The gas turbine operates alongside the wind turbines to ensure a consistent energy supply, especially during low wind periods, providing electricity, heating, cooling, and hydrogen. The system's modular design allows scalability to suit a wide range of residential setups, from single-family homes to multi-story complexes. The design is also flexible enough to integrate alternative renewable sources, such as solar PV or geothermal energy, for regions with differing resource availability.

While wind turbines serve as the primary energy source in the proposed system, their performance is inherently dependent on wind availability, which varies with climatic and geographical conditions. This variability can lead to fluctuations in energy production, particularly during low-wind periods. To address these challenges, the system integrates a gas turbine and hydrogen storage through a PEM

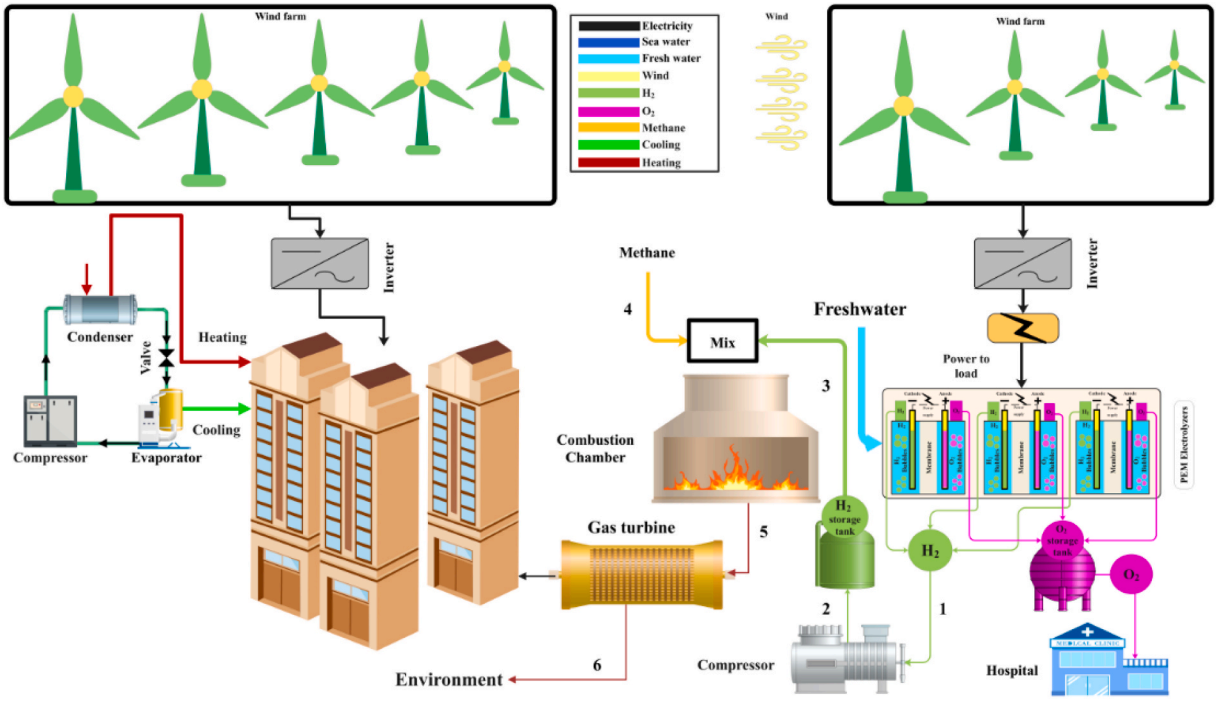

Fig. 1. A schematic of the suggested hybrid system.

electrolyzer. These components act as complementary energy sources, ensuring a consistent energy supply even during periods of low wind availability, thereby enhancing the overall reliability and resilience of the system. While hydrogen storage offers high energy density and scalability for large-scale applications, batteries provide faster response times and higher round-trip efficiency for short-term storage. Supercapacitors excel in applications requiring rapid charge/discharge cycles but are limited in energy capacity. Hydrogen's longer storage duration and ability to integrate with renewable energy sources make it a superior option for achieving large-scale energy resilience in residential ZEBs.

The wind farm, consisting of 28 turbines, is assumed to occupy an area of approximately 4–6 km^2 under optimal spacing conditions. Given the potential distance between the wind farm and the residential building, transmission losses are expected and need to be accounted for in the overall energy performance. While this study focuses primarily on energy production and exergy efficiency, future research should incorporate precise modeling of transmission losses to provide a more realistic assessment.

The system was evaluated using Gothenburg, Sweden, as the case study location to assess its performance. This selection was based on several factors: (1) Gothenburg's geographical characteristics, including consistent wind speeds and temperate climate, which are conducive to wind energy generation; (2) its status as a leader in renewable energy adoption, offering a relevant context for validating the system's application in urban settings; and (3) the variability of climatic conditions in the region, which allowed a comprehensive assessment of the system's adaptability and performance. By analyzing the system in Gothenburg, we ensure its suitability for broader applications in similar urban residential environments.

The electrical energy from the wind turbines is converted into Direct Current (DC) through an inverter and generates hydrogen and oxygen using the PEM electrolyzer through water separation. Hydrogen is directed to the combustion chamber of the Brayton cycle, providing thermal energy for the gas turbine and generating electricity. Meanwhile, the oxygen byproduct can be used for different purposes like utilizing in hospitals. The compression chiller also uses the generated electricity to provide both heating and cooling. By integrating these components, the system offers a versatile solution capable of supplying multiple energy forms, enhancing overall efficiency and sustainability.

3. ANN-based simulation and multi-objective optimization

ANNs machine learning can be used to handle different tasks by learning from data in a way like how the human brain works [41]. These networks enable computers to process information, recognize patterns, and make decisions based on provided data. ANNs are often used in deep learning because of their ability to tackle complex problems using a layered structure. In the context of this study, ANNs offer the practical benefit of accurately modeling complex, nonlinear relationships between input parameters and system outputs, which traditional modeling techniques might not capture effectively.

Neural networks are a powerful tool for handling complex, nonlinear relationships between system parameters and outputs, which are challenging for traditional optimization techniques. In this study, the ANN-based optimization process significantly enhances system efficiency by dynamically predicting the interactions between gas turbine efficiency, wind turbine count, and inlet temperatures. This predictive capability minimizes the need for time-intensive physical experiments, accelerates the optimization process, and identifies configurations that maximize exergy efficiency and minimize costs. By leveraging historical data and simulation results, the neural network adapts to varying operational conditions, ensuring optimal system performance across a wide range of scenarios.

Fig. 2 shows a flowchart of how the neural network method works.

This research pioneers the application of neural networks for optimizing hybrid energy systems, creating a sophisticated model to dynamically balance exergy efficiency and cost under varying operational conditions. This approach overcomes the limitations of traditional optimization methods, offering unprecedented precision in system performance modeling. This dataset was then utilized to train an intelligent ANN, which established a mathematical model to interpret and assess the behavior of the system. The practical benefit here is that the ANN can predict system performance under various conditions without the need for time-consuming and costly physical experiments, thereby accelerating the design and optimization process. The integration of

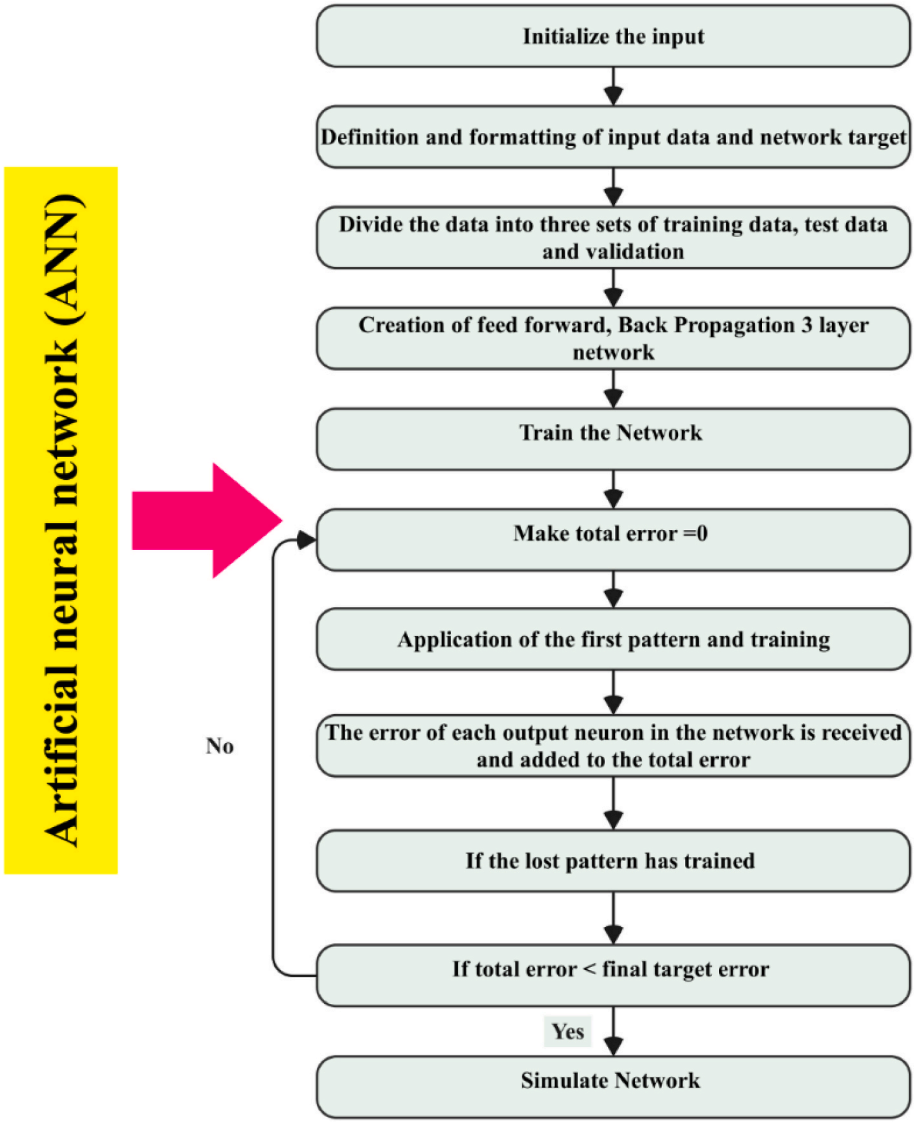

Fig. 2. Flowchart of the ANN

ANN in this study enables predictive capabilities that minimize the need for costly physical experiments, significantly accelerating the optimization process.

Following this, the mathematical model was refined by applying a Multi-Objective Optimization (MOO) using the GA technique, which balanced the input design variables with the output objectives, such as efficiency and cost, to achieve optimal results. GAs provide the practical advantage of efficiently searching through large and complex solution spaces to identify optimal or near-optimal solutions, which might be infeasible with conventional optimization methods. This is particularly beneficial when dealing with multiple conflicting objectives, as GAs can generate a diverse set of Pareto-optimal solutions for informed decision-making. Fig. 3 provides a clear and practical illustration of this intelligent optimization process.

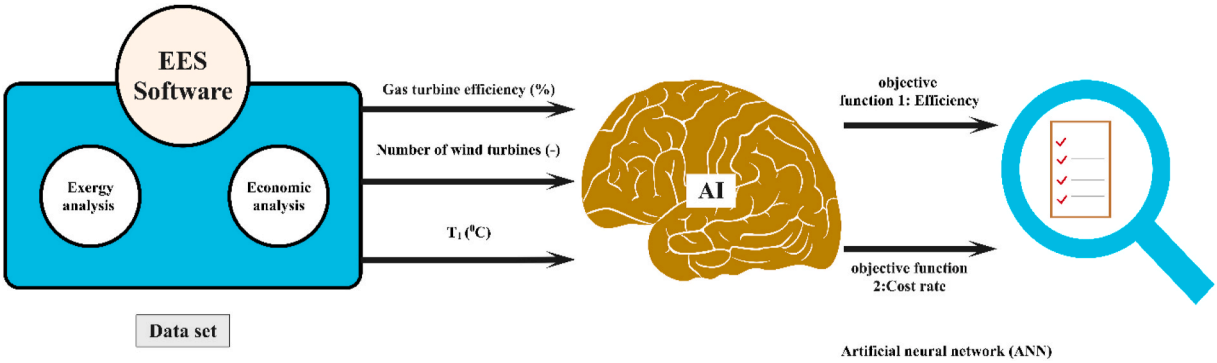

Fig. 3. Structure of the intelligent system optimization process.

4. Governing equations

Energy and mass balance equations are established for every control volume to conduct a comprehensive thermodynamic analysis. For simplicity in the analysis, these assumptions are considered.

1. **Steady-state conditions:** All processes are assumed to occur under steady-state conditions, where system variables such as pressure, temperature, and flow rates remain constant over time. This assumption simplifies the analysis by eliminating the need to model transient dynamics. However, it may reduce accuracy when analyzing time-varying conditions, such as sudden changes in wind availability or load demand, which could impact system performance.
2. **Isentropic turbine:** The gas turbine is modeled as an ideal isentropic process, implying no entropy generation or heat losses. While this assumption is useful for theoretical optimization, it does not account for real-world inefficiencies such as mechanical friction and heat dissipation, potentially leading to an overestimation of turbine efficiency.
3. **Negligible pressure drops in pipelines:** It is assumed that pressure drops in pipelines are negligible. This simplifies calculations and reduces computational requirements but might underestimate the pumping power required in real systems, especially for long or complex pipelines [42].
4. **Insignificant potential energy changes:** The model assumes that changes in potential and kinetic energy are negligible compared to thermal and mechanical energy changes. This is reasonable for flat terrain and moderate flow velocities but may lead to inaccuracies in cases with significant elevation differences or high-speed flows [43].
5. **Insignificant kinetic energy changes:** The model assumes kinetic energy changes are negligible compared to thermal and mechanical energy. This simplification is valid for systems with moderate flow velocities but may lead to slight inaccuracies in high-speed flow scenarios, where velocity variations could affect energy balance and efficiency estimates [43].
6. **Idealized gas turbine efficiency:** The gas turbine is modeled with a combined efficiency of 80%, representing an idealized scenario for modern Combined-Cycle Gas Turbines (CCGT) under optimal operating conditions [44]. This includes both the gas turbine's isentropic efficiency and the additional contribution from a steam turbine utilizing waste heat recovery. While this assumption simplifies the analysis and reflects the upper-performance limit of advanced CCGT systems, it does not account for real-world inefficiencies such as thermal losses, material constraints, and suboptimal operating conditions, which typically reduce efficiency to around 60% in conventional gas turbines.
7. **Neglect of hydrogen compression energy:** The energy required for hydrogen compression to liquid form has been neglected in this analysis to simplify thermodynamic modeling. This assumption focuses on energy flows and system performance but may underestimate overall energy requirements for practical implementation. Future studies should incorporate compression energy demands and multi-stage losses to provide a more comprehensive assessment of the system's efficiency.

These assumptions streamline the modeling process, enabling a more efficient evaluation of system performance while making the model computationally feasible and sufficiently accurate for addressing the aim of this study: optimizing a hybrid energy system for residential ZEBs. The article focuses on assessing energy efficiency and environmental impact rather than capturing transient dynamics or minute inefficiencies, which would significantly increase complexity, computational demands, and data requirements, deviating from the study's primary goal. While these simplifications introduce potential inaccuracies, such as steady-state modeling not fully capturing system responses to fluctuating energy inputs or ideal turbine performance assumptions overestimating exergy efficiency, they allow the model to focus on identifying optimization opportunities and key performance drivers. By balancing analytical tractability and practical applicability, these assumptions align with the article's aim of providing meaningful insights into the system's performance, scalability, and contribution to sustainable energy solutions.

Thermodynamic principles were applied to perform both an economic and thermodynamic assessment of the proposed system [45,46]. This study utilized proposed equation by Refs. [47,48] to calculate energy rates, evaluate the cost-effectiveness of all components, and evaluate the performance of the suggested system. Table 1 describes the inputs for the evaluation of the system. It is important to note that the wind farm, consisting of 28 turbines (n = 28), is assumed to occupy 4–6 km^2 for optimal spacing and performance. While transmission losses due to distance are not included in this analysis, they are acknowledged as an influencing factor in practical applications.

For wind turbines, the aerodynamic efficiency (η_{WT}) represents the maximum theoretical power extraction from wind, limited to 59.3% as per Betz's law, which is the maximum energy that can be extracted from wind. The mechanical-to-electrical conversion efficiency (η_{Gen}) refers to the generator's ability to convert the captured mechanical energy into electrical energy, which is assumed to be 90%. Furthermore, the gas turbine efficiency of 80% represents the CCGT efficiency of modern gas turbine systems operating under ideal conditions, where waste heat recovery significantly improves overall performance.

The wind turbine's area (A_{WT}) is computed based on wind turbine diameter:

$$A_{WT} = \frac{\pi}{4} D^4 \tag{1}$$

The wind turbine generates electricity ($\dot{W}_{WT}$) is calculated as below [31]:

$$\dot{W}_{WT} = \frac{1}{2} \times \eta_{\mathrm{WT}} \times \rho_{air} \times A_{WT} \times \eta_{\mathrm{ecoefficiency}} \times V_{wind.speed}^3 \times \frac{4}{1000} \tag{2}$$

where η_{wt} is the wind turbine efficiency and ρ_{air} is the air density. Given that the wind farm is made up of several wind turbines, its production power is determined as:

$$\dot{W}_{WindFatm} = n \times \dot{W}_{WT} \tag{3}$$

The system's overall net power value is

$$\dot{W}_{net} = \dot{W}_{GT} + \dot{W}_{WindFarm} + \dot{W}_{Chiller} + \dot{W}_{PEM} \tag{4}$$

It should be noted that the amount of electricity consumed by the electrolyzer is calculated as

$$\dot{W}_{PEM} = 0.2 \times \dot{W}_{WindFatm} \tag{5}$$

The compression chiller's electrical usage is

Table 1
Input data for system analysis.

Parameter	Description	Value
Wind turbine		
V (m/s)	Mean wind speed	5
η_{WT} Aerodynamic (%)	Wind turbine aerodynamic efficiency (Betz's limit)	59
η_{Gen} Mechanical-Electrical (%)	Wind turbine generator efficiency	90%
n (—)	Number of wind turbines	28
D (m)	Wind turbine diameter	34
Gas turbine		
$GT_{efficiency}$ (%)	Gas turbine efficiency	80
T_0 (°C)	Outdoor temperature	25
P_0 (kPa)	Ambient pressure	101.3

$$\dot{W}_{Chiller} = 0.2 \times \dot{W}_{net} \tag{6}$$

Overall exergy efficiency is determined as follows

$$\eta_{\dot{E}x} = \frac{\dot{W}_{net} \times 100}{\dot{E}x_{WindTurbine}} \tag{7}$$

The overall components' investment cost (Z) is calculated as

$$Z_{total} = Z_{Chiller} + Z_{PEM} + Z_{WindTurbine} + Z_{CC} + Z_{GT} \tag{8}$$

Table 2 presents the relationships between every component cost and the intended auxiliary relations.

5. Results and discussion

The proposed hybrid system's performance is evaluated through thermodynamic and economic analyses. Each component, including wind turbines, gas turbines, the PEM electrolyzer, and the compression chiller, is assessed for its contribution to overall energy output and cost. By integrating renewable energy with gas turbine technology, the system ensures continuous power generation, overcoming the intermittency of wind energy, achieving an energy efficiency of 33.69% and an optimized exergy efficiency of 36.95%. Optimization through ANN modeling and genetic algorithms further enhances efficiency and cost-effectiveness. The following sections will focus on validation, optimization results, and system performance analysis.

5.1. Validation of the proposed system

Before analyzing the proposed system, validation was conducted to confirm the accuracy of the results. Due to the system complexity, the PEM electrolyzer subsystem was justified by comparing the modeling results with the experimental findings of Ioroi et al. [49]. The comparison was conducted under the same operational conditions (e.g., input temperature, pressure, and current density) as the benchmark study. The close agreement between the simulated exergy efficiency and the experimental data demonstrates the reliability of the modeling framework. Fig. 4 illustrates this comparison, highlighting the accuracy and reliability of the simulation and enhancing confidence in the overall simulation framework used in this study. This validation step ensures the accuracy and applicability of the proposed system model for predicting real-world performance.

5.2. System performance optimization

The MOO was carried out using a neural network-based approach to enhance overall system performance and minimize operational costs. The main goal of the optimization was to enhance exergy efficiency while minimizing the cost. The optimization variables and their corresponding ranges were selected based on practical considerations, technological constraints, and the potential impact on system performance. These ranges represent a balance between realistic operating conditions and the boundaries required to explore optimization possibilities. By examining these variables within the specified limits, the study ensures

Table 2
Cost balance and Supporting Relationships.

System Component	Equation
Wind turbine	$Z_{WindTurbine} = 5000 \times W_{WindFarm}$
PEM	$Z_{PEM} = FFFF \times 1000 \times \dot{W}_{PEM}$
Combustion chamber	$Z_{CC} = \frac{(48.64 \times \dot{m}_i)}{\frac{0.92 - P_0}{P_i}} \times (1 + \exp(0.018 \times T_0 - 26.4)$
Gas turbine	$Z_{GT} = \left(\frac{1536 \times \dot{m}_g}{0.92 - \eta_{GT}}\right) \times ln\left(\frac{P_i}{P_0}\right) \times (1 + \exp(0.036 \times T_i - 54.4)$
Compression chiller	$Z_{Chiller} = 1144.3 \times (Q^{0.67})$

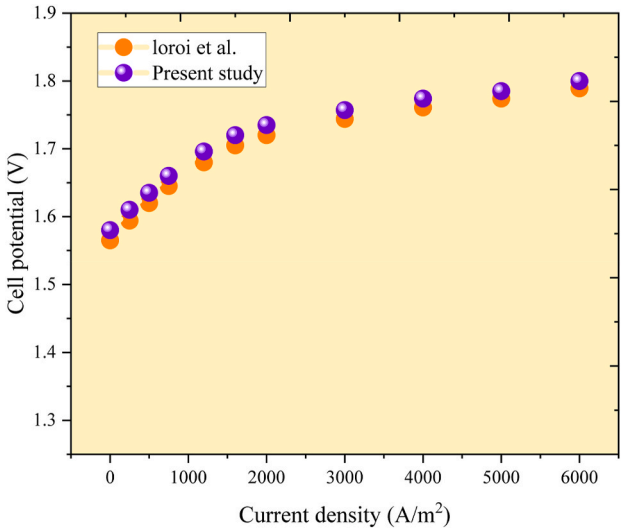

Fig. 4. Validation of the PEM electrolyzer subsystem.

the applicability of the results to real-world systems while maintaining the flexibility to identify optimal configurations. Table 3 outlines key optimization variables along with their respective ranges, providing a basis for fine-tuning the system's performance.

The ideal values for the goal functions and decision factors are shown in Table 4, providing critical insights into potential improvements. Data were extracted from system modeling, simulating interactions between components like wind and gas turbines, and the PEM under various conditions. The chosen ranges for the optimization variables have practical implications for the system design. For instance, gas turbine efficiency (70%–95%) reflects advancements in turbine technology, with higher efficiency reducing energy losses at the cost of increased investment in advanced materials and designs. The range for the number of wind turbines (10–40) allows for scalability while considering economic and spatial constraints. Similarly, the turbine inlet temperature range (1000–1200 K) represents operational limits that optimize thermal efficiency without risking material degradation. These ranges provide a foundation for exploring trade-offs between performance, cost, and feasibility in the optimization process. The problem was addressed using a neural network to model nonlinear relationships, followed by optimization with Genetic Algorithms. This approach explores the solution space, ensuring practical, optimal configurations and highlighting potential enhancements in system performance and cost-effectiveness.

The integration of neural networks in the optimization process demonstrated significant improvements in system performance. By accurately modeling complex interactions among design parameters, the ANN-based optimization achieved an exergy efficiency of 36.95% and a cost rate of $446.04 per hour. Compared to traditional hybrid energy systems, this approach reduced computational overhead and identified Pareto-optimal solutions that balance efficiency and cost. The ability to adapt to fluctuating operational conditions further underscores the neural network's role in ensuring consistent and enhanced system efficiency.

Fig. 5 presents the range of variations during the optimization process, highlighting optimal values for every function.

Fig. 5 demonstrates a clear trade-off between cost rate and exergy

Table 3
Optimization variables and ranges.

Parameter	Lower limit	Upper limit
Gas turbine efficiency (%)	70	95
Number of wind turbine (—)	10	40
T_5 (^0K)	1000	1200

Table 4
Optimized values of objective functions and decision variables for system performance.

Parameter	Optimum point	Minimum	Maximum	Std. Dev.	Run
T_5 (^0K)	1165.04	1000	1300	82.82	500
Gas turbine efficiency (%)	82	0.7	0.95	0.07	500
Number of wind turbine (−)	25	10	40	8.52	500
Exergy efficiency (%)	36.95	18.28	80.77	14.51	500
Cost rate ($/h)	446.04	7.85	978	169.65	500

efficiency, with the Mean ± SD range for cost rate spanning between $300/h and $620/h, while exergy efficiency varies between 20 and 50%. The wider variability observed in the Mean ± 1.96*SD range for cost rate compared to exergy efficiency highlights the system's sensitivity to external parameters and optimization constraints. This suggests that cost optimization is more dynamic and influenced by a broader set of variables, whereas exergy efficiency demonstrates relatively stable bounds. It provides valuable insights for guiding system design, enabling stakeholders to prioritize either cost reduction or performance enhancement based on specific application requirements.

The Pareto diagram for objective functions is presented in Fig. 6. In the MOO process, the Pareto optimal solutions are identified, indicating the optimal balance between the two competing objective functions. This diagram illustrates how the optimization problem is resolved by simultaneously optimizing both functions, highlighting the balance between them. The Pareto front depicted in the figure shows how improvements in one objective necessitate compromises in the other, emphasizing the inherent trade-off between cost rate and exergy efficiency. The strong correlation (R^2 = 0.96119) reflects a well-defined relationship, where higher exergy efficiencies are generally associated with reduced costs, although achieving the ideal range of 70–80% efficiency at around $100/h cost rate remains challenging.

Fig. 6 shows that the STATISTICA-selected point (30–40% exergy efficiency at $400–450/h cost rate) prioritizes moderate efficiency levels with higher costs, deviating from the ideal trade-off zone. This highlights the need for additional constraints or objective weighting to guide the optimization process closer to the desired balance. The visualization provided by the Pareto front helps stakeholders understand these trade-offs and select solutions that align with system goals, emphasizing the potential for further refinement of the optimization model to enhance its applicability to real-world scenarios.

Fig. 7 illustrates the histograms that show the overall results from the training and calculation processes. The height of each column corresponds to the frequency of the respective value.

The observations indicate that most exergy efficiency values fall between 20–30% and 30–40%, with significantly fewer occurrences at extreme ranges (10–20% and 80–90%), suggesting a concentration of optimization outcomes in moderate efficiency levels. Similarly, for the cost rate, the highest frequency is observed to be between 400 ($/h) and 600 ($/h), followed by 200($/h) to $400 ($/h), while values above 900 ($/h) are rare. These patterns reflect the optimization process's tendency to prioritize solutions that balance cost and efficiency, avoiding extreme values that might compromise feasibility.

Fig. 8 presents the normality plot for exergy efficiency and wind farm cost rate, illustrating the normal distribution of residuals from the linear regression. For exergy efficiency (%), most data points align closely with the regression line, with minor deviations indicating slightly reduced accuracy compared to the cost rate. For cost rate ($/h), residuals follow a normal distribution with broader variability, reflecting higher sensitivity. The alignment with the normal distribution validates the model's reliability in balancing these objectives within the system design.

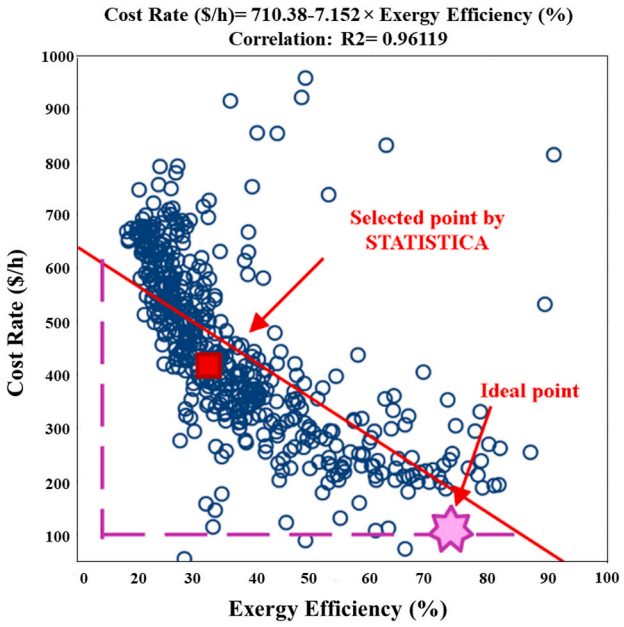

Fig. 6. Pareto diagram: Trade-offs between objective function.

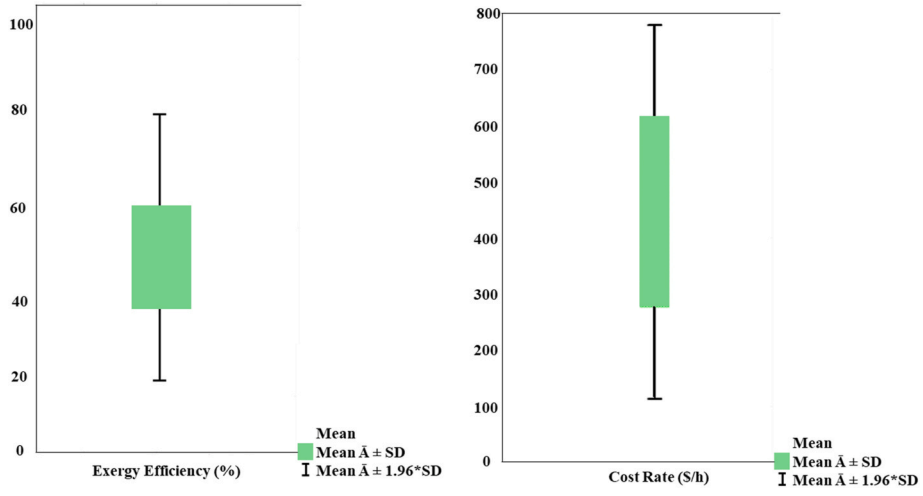

Fig. 5. Trade-offs between objective function during optimization procedure.

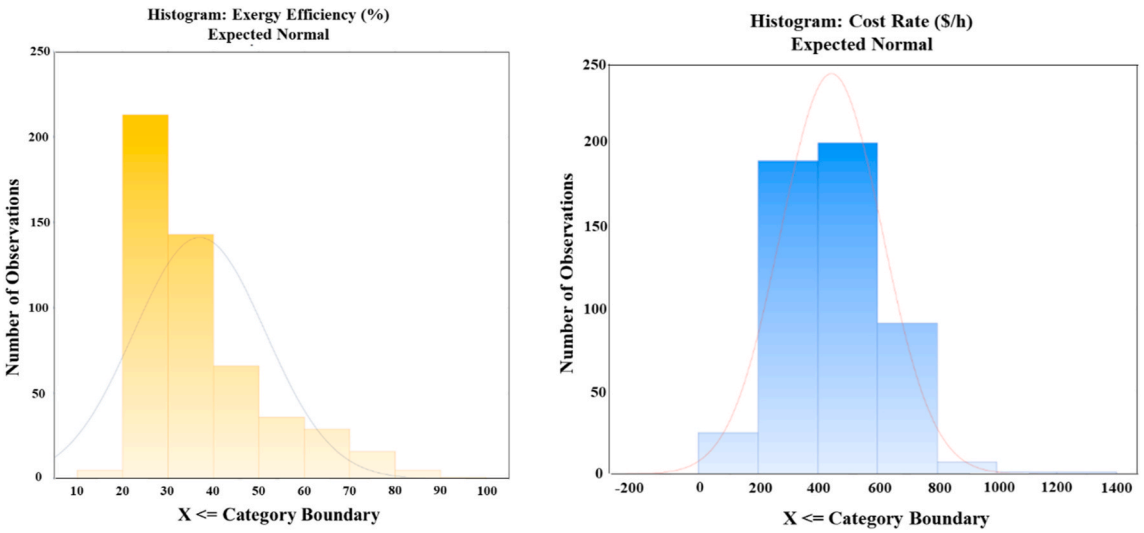

Fig. 7. Histograms of frequency distributions for objective functions.

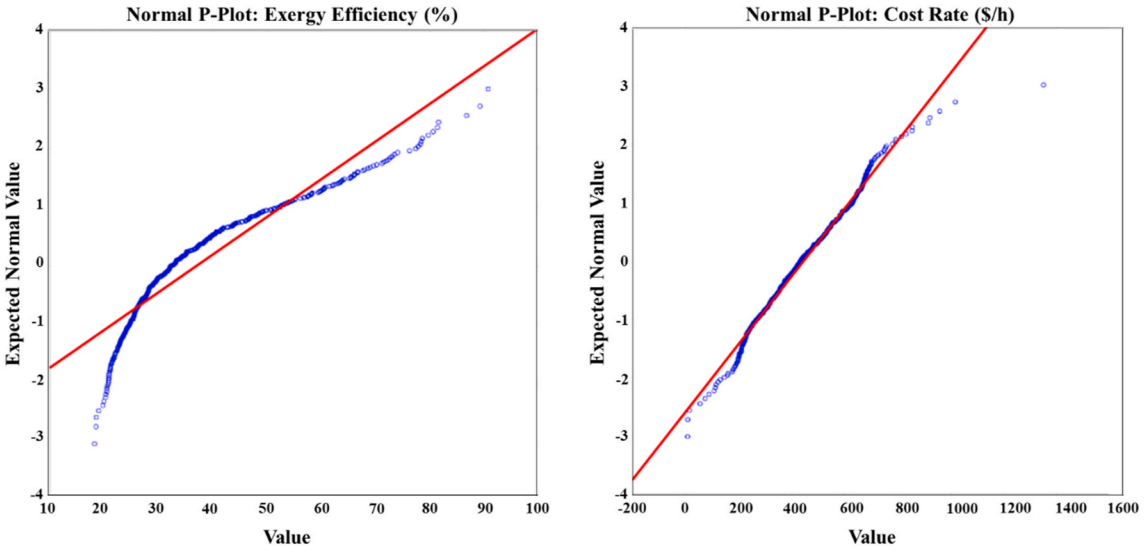

Fig. 8. Normality plot of objective functions.

Fig. 9 depicts expected normal values for objective functions, illustrating the expected distribution of these values as determined by the optimization and regression analysis. The Half-Normal P-plot for exergy efficiency (%) shows a strong linear trend, with data points particularly well-aligned with the regression line for values under 200 and over 650, indicating reliable model predictions and robust optimization of the relationship with system parameters in these ranges. Similarly, the plot for cost rate ($/h) displays a generally linear trend, though with a narrower range, reflecting accurate predictions but greater sensitivity in cost optimization. The alignment of residuals with the expected distribution validates the model's effectiveness in balancing performance and cost efficiency, consistent with the objectives of this study.

Fig. 10 compares predicted versus actual values, evaluating the model's accuracy. The alignment of data points with the regression line for each objective function highlights reliable predictions across the range for exergy efficiency (%), as the regression line exhibits a strong linear trend. For cost rate ($/h), the regression line also aligns well, though with slight deviations at the extremes, reflecting higher variability. This alignment between predicted and actual values validates the model's effectiveness in balancing and optimizing both objectives.

Fig. 11 plots the raw residuals against the actual values that highlight the discrepancies between these values, offering insights into the accuracy and performance of the predictive model. The horizontal red line at 0 residual represents the ideal alignment between predicted and actual values, with the clustering of residuals near this line for both objectives demonstrating the model's effectiveness. Conversely, the wider spread of residuals at the extremes reflects increased variability, indicating areas where further refinement of the model could enhance prediction accuracy.

Fig. 12 illustrates the decision variables' influence on the exergy efficiency. The performance of the system is significantly influenced by the wind turbines and gas turbines, the critical components. By increasing wind turbines from 10 to 40, exergy efficiency decreases from 60% to 20%. This decline occurs because adding more wind turbines increases the total energy input from wind, but the system's ability to efficiently utilize this energy diminishes due to limitations in downstream components, such as energy conversion systems and storage capacities, leading to higher exergy destruction. In contrast, increasing the efficiency of the gas turbine from 70% to 95% enhances efficacy from 32% to 40%. This improvement is attributed to reduced energy losses in the turbine, as higher efficiency minimizes irreversibility in the combustion and energy conversion processes, resulting in better

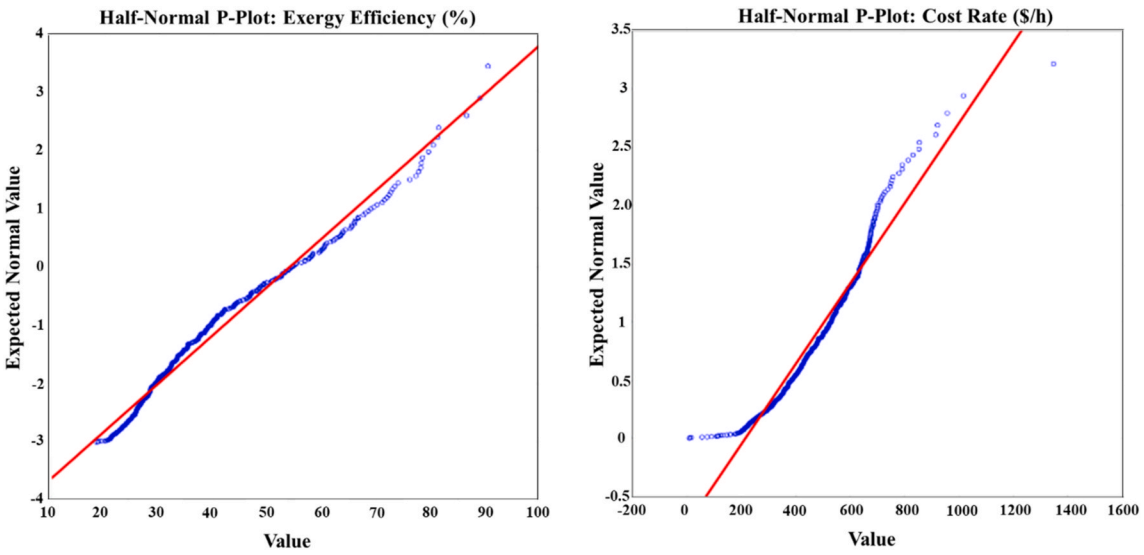

Fig. 9. Expected normal distribution of objective functions.

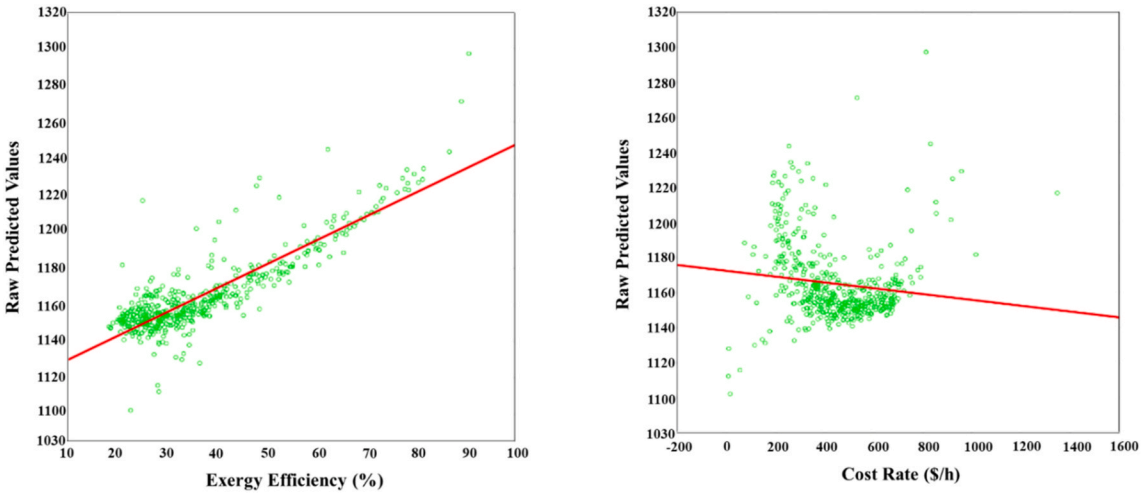

Fig. 10. Predicted vs. Actual Values for Objective Functions.

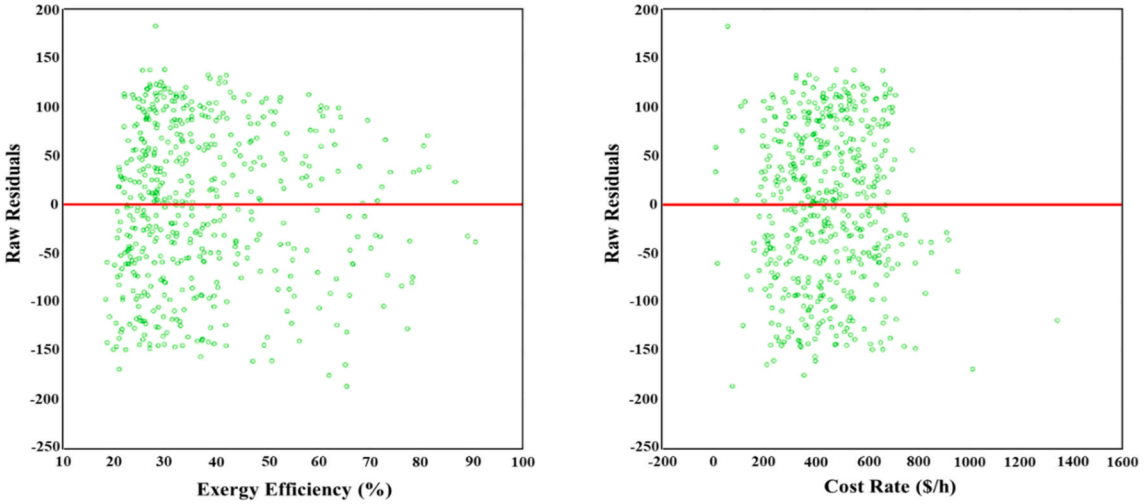

Fig. 11. Residuals vs. Actual Values for Objective Functions.

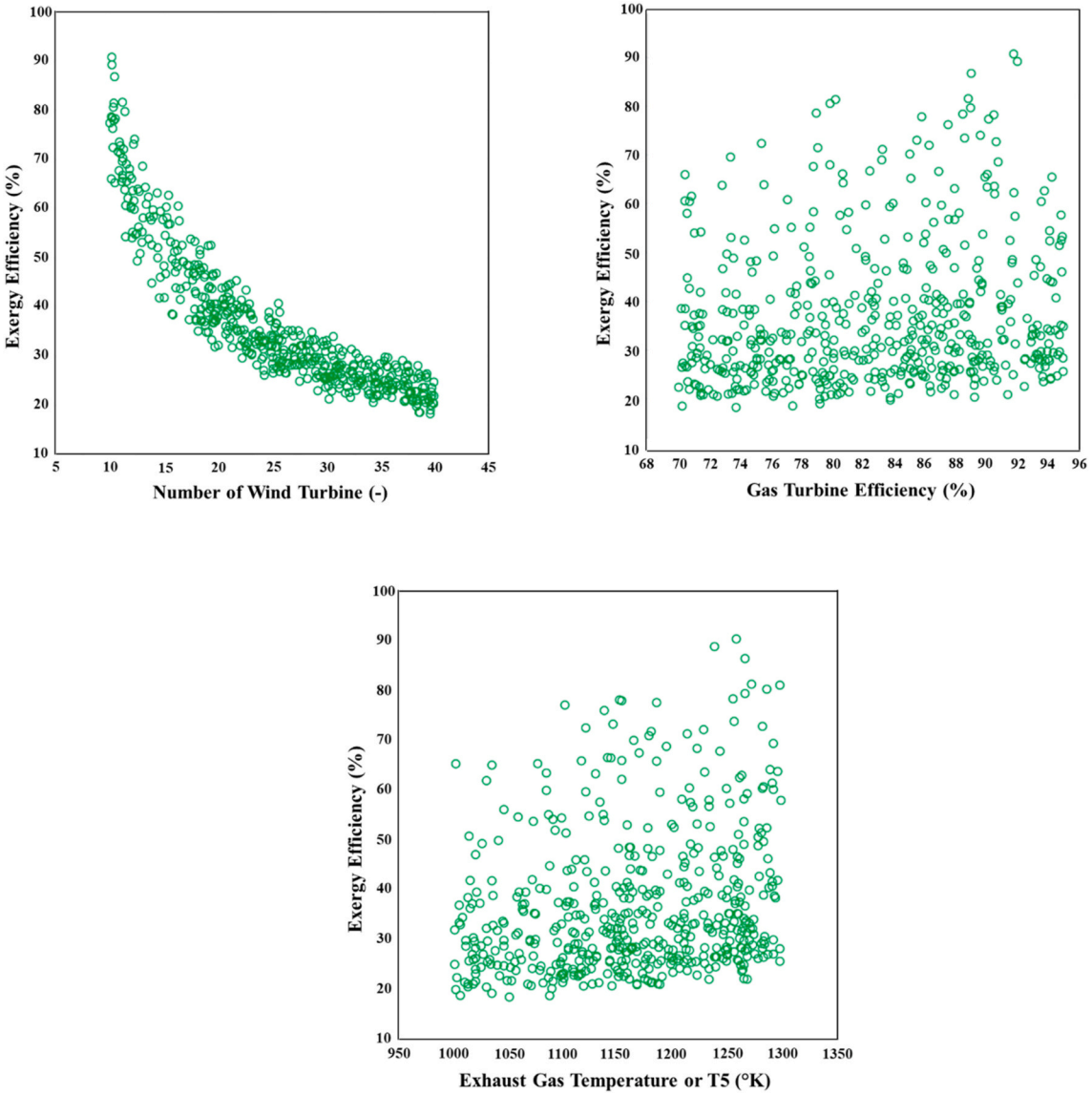

Fig. 12. Decision factors impacts on exergy efficiency.

utilization of available energy. Load distribution graphs show how exergy efficiency varies with different decision variables. The parametric analysis is performed in optimization mode, where all influencing parameters are considered simultaneously. Besides the parameter on the horizontal axis, two other variables are also impacting exergy efficiency.

Fig. 13 demonstrates the effect of key decision factors on the cost, highlighting wind and gas turbines as the main contributors to the system's overall economic costs. Increasing the number of wind turbines from 10 to 40 raises operating costs from $200 to $630 per hour, driven by higher capital, maintenance, and storage requirements. Similarly, increasing the efficiency of the gas turbine from 70% to 95% raises costs from $410 to $420 per hour due to the need for advanced technologies and materials that reduce energy losses but incur higher operational expenses. In contrast, raising the gas turbine temperature from 1000 °C to 1300 °C slightly lowers cost from $430 to $420 per hour by improving thermal efficiency, reducing fuel consumption, and offsetting maintenance expenses.

5.3. Exergy and component performance

Exergy analysis provides a deeper understanding of the energy quality within the system, identifying inefficiencies and energy losses. By evaluating the exergy destruction across various components, it becomes possible to highlight areas for improvement and further optimize system performance.

5.3.1. Wind farm performance

The wind farm, consisting of 25 turbines, demonstrates impressive electricity generation capabilities. It supplies 4745 kWh to the grid and an additional 948 kWh to the PEM electrolyzer for generating hydrogen and oxygen. However, the wind turbines themselves destroy 730 kWh of exergy during the process.

5.3.2. Hydrogen and methane production

The PEM uses 948 kWh to generate 10 kg/h of hydrogen. The PEM electrolyzer operates at an optimal temperature of 80 °C and produces hydrogen at a pressure of 3000 kPa, selected to ensure compatibility with downstream combustion processes while minimizing the need for additional compression. For every kilogram of hydrogen generated, approximately 9 L of water are consumed. The system's design ensures that water supply and operational temperature are maintained to optimize performance.

Two scenarios for fuel input to the combustion chamber were analyzed: pure hydrogen and a hydrogen-methane mixture. In the

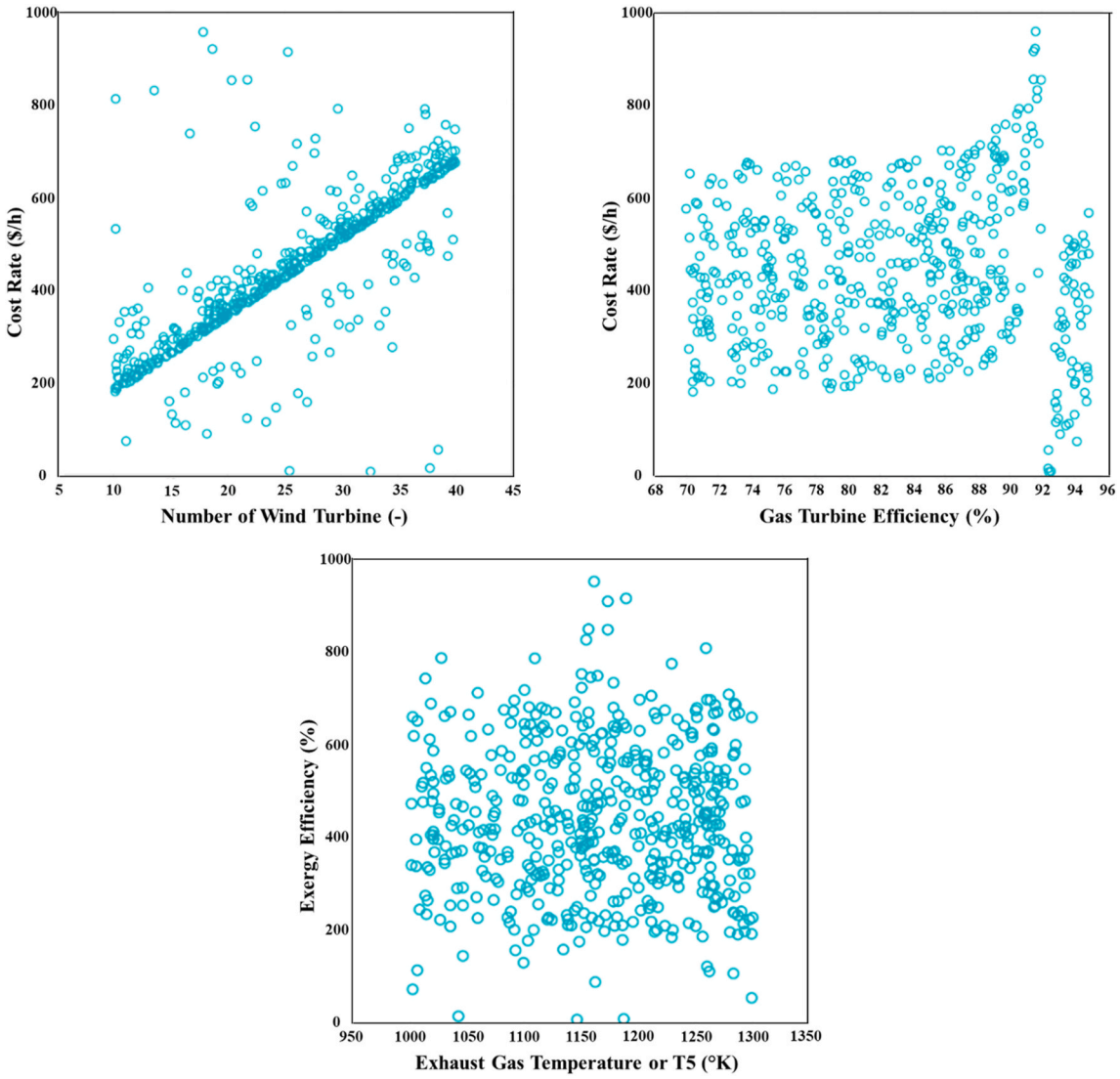

Fig. 13. Impact of decision variables on cost rate-related choice variables.

hydrogen-methane mixture scenario, the hydrogen, combined with 1018 kg/h of methane, was assumed to be derived from existing natural gas supply chains for transitional purposes. This mixture is fed into a mixer and subsequently into the combustion chamber to generate thermal energy for the gas turbine. Methane production in this scenario is assumed to align with cost-effective pathways, such as existing natural gas infrastructure, making it viable for transitional purposes but not considered a long-term solution for net-zero systems due to its reliance on methane. While combustion processes are effective for generating thermal energy, hydrogen fuel cells offer a cleaner alternative by directly converting chemical energy into electricity through an electrochemical reaction. This eliminates heat pollution, enhances system efficiency, and minimizes environmental impacts.

During this process, the PEM electrolyzer destroys 933 kWh of exergy. This exergy destruction highlights the need for optimization in PEM electrolyzer design to improve overall system efficiency. While the hydrogen-methane mixture demonstrated potential for cost reduction, pure hydrogen was prioritized as the preferred fuel due to its higher combustion efficiency and environmental benefits, aligning more closely with sustainable energy goals.

5.3.3. Gas turbine efficiency

The gas turbine uses the heated mixture from the combustion chamber to generate electricity but incurs an exergy destruction of 509 kWh and consumes 245 kWh of electricity in the process.

5.3.4. Overall system performance

In summary, the system destroys a total of 2037 kWh of exergy per hour of operation, indicating significant energy losses and inefficiencies. By analyzing the exergy diagram and destruction rates, engineers can pinpoint areas for optimization. Fig. 14 illustrates energy performance evaluation, detailing each component's energy flow.

In operational terms, the observed exergy destruction across system components (2037 kWh), signifies critical inefficiencies that must be addressed to optimize system performance. For example, the wind turbines, responsible for generating the majority of the system's energy, exhibit significant exergy destruction (730 kWh), suggesting the need for improved aerodynamic designs or advanced control systems to enhance energy conversion efficiency. Similarly, the PEM electrolyzer, which incurs 933 kWh of exergy loss, highlights the potential for advancements in material science and electrode design to reduce energy waste during hydrogen production.

The implications of these inefficiencies extend beyond energy performance, as higher exergy destruction in the gas turbine (509 kWh) reduces both thermal efficiency and impacts the overall reliability and scalability of the system. Addressing these losses through strategies such

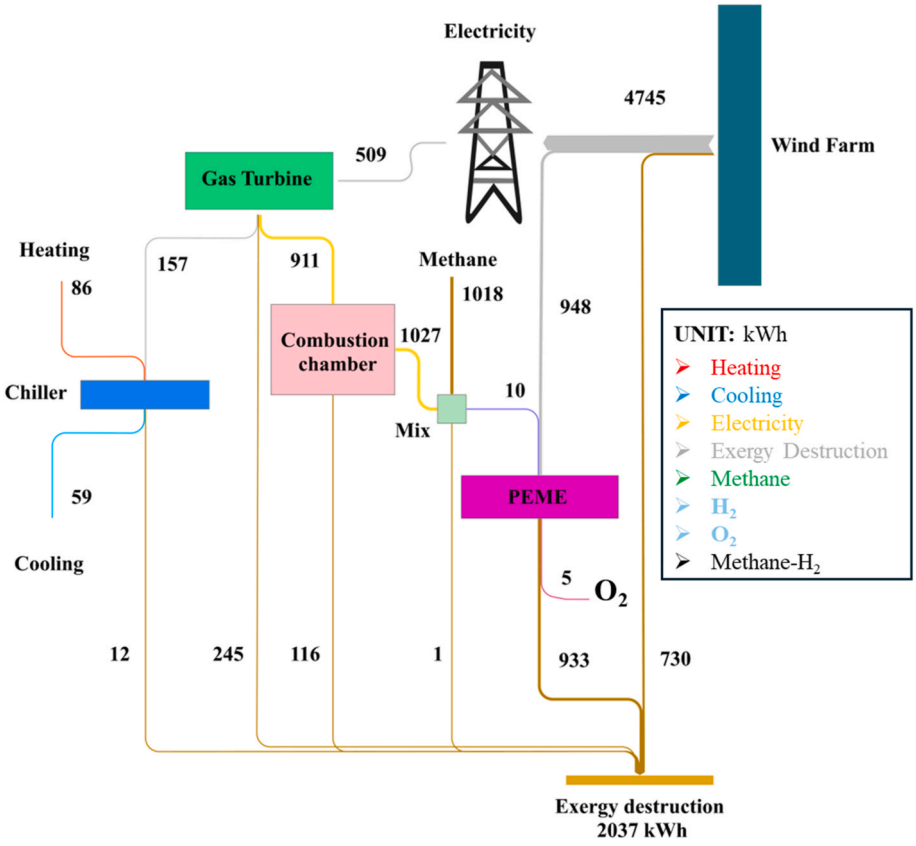

Fig. 14. Analysis of system energy.

as optimizing turbine inlet temperature or integrating more efficient heat recovery systems could considerably enhance performance. From a practical perspective, mitigating exergy destruction is essential for improving the system's economic viability and environmental sustainability. Lowering these inefficiencies will reduce operational costs, enhance reliability, and create a better balance between renewable energy input and end-use energy delivery, ultimately supporting the achievement of ZEB goals and advancing the transition to sustainable energy systems.

5.4. Environmental performance

The proposed system achieves a CO_2 reduction of 10,416 tons annually, a significant improvement compared to traditional hybrid systems and other systems reported in the literature. Table 5 highlights a comparative analysis between the present study and previously published results.

Table 5 highlights that the proposed system outperforms other systems in key areas. With an annual CO_2 reduction of 10,416 tons, it far exceeds reductions reported in previous studies, which achieved only 23.3 tons/year [52] and 2800 tons/year [56]. This improvement is

Table 5
Comparative analysis of the proposed system and traditional hybrid systems.

Ref	System Description	Optimization Method	Cost of Energy	Efficiency (Energy/Exergy)	CO2 Reduction (tons/year)
Present study	Hybrid system: wind turbines, gas turbines, PEM electrolyzers.	ANN-based MOO	$0.88/kWh	33.69%/36.95%	10,416
[50]	Gas turbine with heat recovery, hydrogen blending.	MOO	$1.514/h	Exergy from 31.34% to 42.73%	Not provided
[51]	Solar & geothermal hybrid: Rankine cycles, absorption systems, and hydrogen storage.	Energy & exergy analysis	Not provided	83.28%/58.71%	3.351 kg CO_2/kWh avoided
[52]	Solar-based multi-generation system with hydrogen storage & PV panels for 4 climates in Iran.	Multi-objective optimization (TOPSIS)	$6.08/h (lowest)	26.3% (exergy, Bandar Abbas)	Bandar Abbas: 23.3 tons, Yazd: 4.4 tons
[53]	Solar-wind hybrid multi-generation with TES, RO, ICE, and HESS in 4 Russian cities.	Dynamic simulation with TRNSYS, EES, EnergyPlus	Not provided	33.51%/27.07% (Khabarovsk)	Khabarovsk: 20.34 tons, Yakutsk: 5 tons
[54]	Flexible load-regulated hybrid cooling, heating, power system for Shanghai households.	4E analysis (energy, exergy, environmental, economic)	Hydrogen: $1.557/kg (target cost)	Winter: 89.21%/58.04%; summer: 73.26%/55.47%	Winter: 67.26%; summer: 67.43%
[55]	Renewable energy-based multi-generation for residential complexes, including solar & hydrogen storage.	Thermodynamic modeling	Not provided	36%/44%	476
[56]	Hybrid energy systems: PV/Wind/Diesel and PV/Wind/Battery for Jubail residential compounds in Saudi Arabia.	HOMER optimization	$0.183–0.25/kWh	Not provided	2800

primarily attributed to the integration of advanced components such as wind turbines, gas turbines, and PEM electrolyzers, combined with an ANN-based MOO approach that ensures efficient energy conversion and minimal emissions. While some studies report notable relative CO_2 avoidance (3.351 kg CO_2/kWh) [57], the absolute impact of those systems is limited by their scale. The proposed system also achieves a highly competitive energy cost of $0.88/kWh, which is more cost-effective than some previous systems with $1.514/h [50] comparable to fully renewable configurations ($0.183–$0.25/kWh) [56]. The optimized design, including effective heat recovery and hybrid energy management, contributes to reducing operational costs.

The energy and exergy efficiencies of the proposed system are also noteworthy (33.69% and 36.95%), demonstrating comparable or superior performance to other hybrid systems. Some of the previous studies report slightly higher efficiency levels in specific seasonal or climate-dependent conditions (36% and 44%) [54], but the proposed system's robust, year-round scalability and integration of hydrogen as an energy carrier ensure its adaptability to varying load demands, enhancing its overall efficiency and sustainability. These findings highlight the proposed system's balanced approach, combining advanced technology, high environmental impact, and economic feasibility, making it a model for sustainable energy solutions in residential applications.

5.5. Economic analysis

Fig. 15 shows the cost rates distribution among five main components: PEM electrolyzer, gas turbine,the wind farm, combustion chamber, and compression chiller unit. The total operating cost is $446.04 per hour. The wind farm, consisting of 25 turbines, represents the highest cost contributor, with an expense rate of $396.7 per hour. Following this, the gas turbine contributes $18.9 per hour, while the PEM electrolyzer, responsible for hydrogen and oxygen production, encounters a cost rate of $15.87/hour. The compression chiller unit costs $10.91 per hour, and the combustion chamber has the lowest cost rate at $3.66 per hour. In regions offering incentives for renewable hydrogen production or wind energy development, such as the European Union or the United States, the economic feasibility of the proposed system could be further enhanced. Aligning the system's design with such policies would accelerate its adoption and scalability.

5.6. Case study analysis

In this research, the designed system is examined within the context of Sweden, a country in continental Europe. The technical, economic, and environmental performance is analyzed across four Swedish cities: Kalmar, Gothenburg, Stockholm, and Sundsvall to evaluate its adaptability to different climatic conditions. These cities represent diverse Swedish climates, ranging from southern coastal (Kalmar) to northern inland (Sundsvall) environments. This analysis ensures the system's robustness, scalability, and effectiveness across varying weather conditions and energy demands. Fig. 16 provides a geographical map of Sweden, highlighting the cities under investigation.

Fig. 17 shows the monthly variations of ambient temperature and wind speed for the selected cities, reflecting diverse climatic conditions. Sundsvall, representing northern inland Sweden, experiences the coldest temperatures, with averages as low as −5.73 °C in February, while Gothenburg, located on the southwest coast, records the warmest conditions, peaking at 24.45 °C in July. Kalmar and Stockholm exhibit moderate variations between these extremes. Wind speed variations further emphasize significant energy potential across the cities, with Kalmar and Gothenburg showing higher monthly averages, such as 4.24 m/s in January for Kalmar and 5.19 m/s in April for Gothenburg. In contrast, Sundsvall and Stockholm experience moderate wind speeds, ranging from 2.34 to 3.94 m/s throughout the year. These variations highlight the climatic diversity of the selected regions and underscore their suitability for evaluating wind energy potential and hybrid energy system performance.

Fig. 18 illustrates the monthly variations in average net power generation for the gas turbine, wind farm, and the overall system across four selected cities, in response to varying weather conditions, specifically wind speed and outdoor temperature. The results indicate that Gothenburg and Sundsvall exhibit the highest gas turbine outputs. However, Sundsvall records the lowest wind farm output (below 2500 kWh monthly average) among four selected cities, which is expected due to its low average wind speed, particularly during winter, shown in Fig. 17. In contrast, Gothenburg achieves the highest wind farm output (exceeding 8000 kWh monthly average), especially in April, when the average wind speed reaches 5.19 m/s (refer to Fig. 17). Stockholm and Kalmar show comparable gas turbine outputs (ranging between 750 and 780 kWh), while Kalmar demonstrates superior wind farm performance, except between September and December when outputs are nearly equal. Overall, the total power generation highlights Gothenburg as the top performer, delivering approximately 35% higher total output compared to Kalmar, the second-best city.

Fig. 19 illustrates the monthly variations in heating and cooling production influenced by changing weather conditions. Heating production remains relatively stable, with Gothenburg and Sundsvall consistently achieving the highest output (around 600 kWh monthly average) and Stockholm and Kalmar slightly lower (approximately 540 kWh). Similarly, cooling production shows similar trends, closely mirroring gas turbine electricity generation since the compression chiller unit is powered by the turbine, with 20% of its output allocated to cooling. As a result, Gothenburg and Sundsvall lead in cooling output (exceeding 430 kWh), while Stockholm and Kalmar follow at around 390 kWh. These patterns highlight the interdependence between gas turbine performance and cooling production, driven by seasonal and

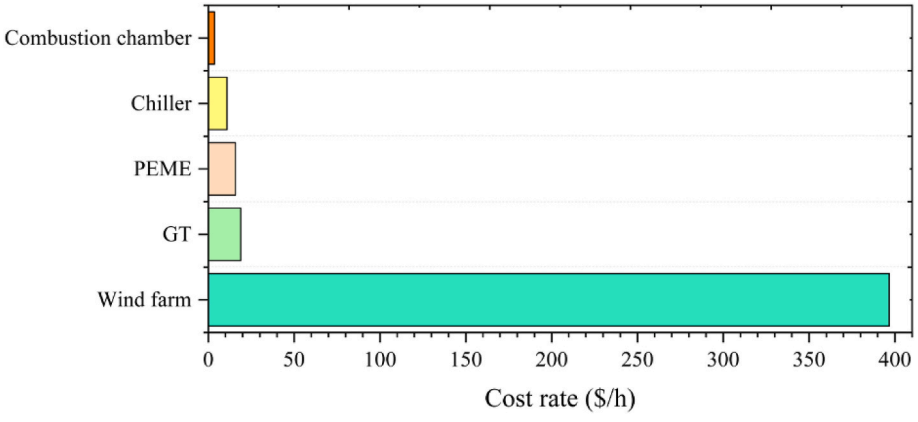

Fig. 15. Cost rate distribution of system components.

Fig. 16. Map of Sweden showing the cities analyzed.

operational fluctuations.

Fig. 20 displays the changes in monthly average of oxygen and hydrogen generation over a year, in response to varying meteorological conditions. This figure shows Gothenburg leading in both oxygen and hydrogen production throughout the year. Gothenburg consistently achieves the highest generation levels, peaking in April (8.18 kg/h oxygen, 16.35 kg/h hydrogen). This can be attributed to Gothenburg's favorable wind speeds and temperate climate, which enhances wind turbine performance and ensures a stable energy supply to the PEM electrolyzer. The integration of wind power with hydrogen production aligns with the study's focus on addressing intermittent renewable energy through hybrid energy systems, enabling continuous energy generation and storage. Seasonal variations in production highlight the system's adaptability to local meteorological conditions, while the optimized design maximizes energy utilization, particularly during high-wind periods in spring.

Fig. 21 displays monthly variations in average cost rate ($/h) due to weather conditions (i.e., wind speed and temperature). Gothenburg, with the highest rate, shows substantial fluctuations, peaking in April (740.01 $/h) due to its reliance on wind-driven energy production and seasonal meteorological changes. Kalmar exhibits the second-highest cost rates, with a peak in January (455.99 $/h), likely driven by higher energy demands during colder temperatures. Sundsvall consistently maintains the lowest average cost rates, with a slight increase in June (288.23 $/h) reflecting seasonal variations in wind energy supply. Stockholm experiences moderate cost rates throughout the year, rising in January (383.13 $/h) and December (337.86 $/h) due to increased energy demands during winter. These variations underscore the critical impact of regional and seasonal weather conditions on energy generation costs, emphasizing the need for adaptive cost optimization strategies in hybrid energy systems.

The results of evaluating the designed hybrid energy system across

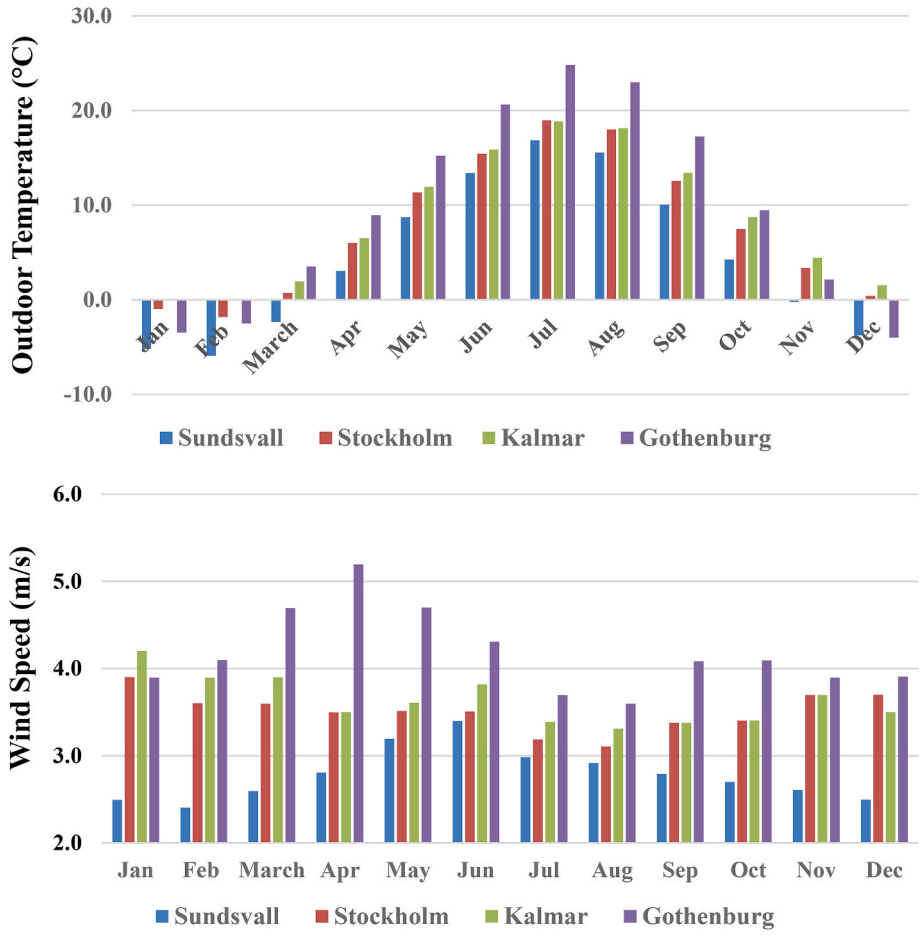

Fig. 17. Monthly variations of ambient temperature and wind speed in the selected cities.

four selected Swedish cities highlight Gothenburg as the top-performing location due to its higher wind speeds and favorable meteorological conditions, achieving the highest outputs in wind farm generation, gas turbine production, and energy outputs for hydrogen, oxygen, heating, and cooling. Kalmar follows the second-best in wind farm and total energy output, as well as in oxygen and hydrogen generation. Sundsvall emerges as the second-best in gas turbine output and heating and cooling generation, showcasing strong performance despite its lower wind resources. Stockholm and Kalmar exhibit similar outputs in heating and cooling generation, with Stockholm showing moderate overall performance. This section underscores the system's adaptability to varying climatic conditions, balancing renewable energy generation with cost-efficient outputs across energy, heating, cooling, and gas turbine systems. The findings demonstrate the system's scalability and its potential to achieve zero-energy goals in residential applications across regions with varying renewable energy potential.

5.7. Energy production and environmental analysis

Fig. 22 compares annual electricity, cooling, and heating production across the four selected cities. The figure highlights that Gothenburg leads in total energy production (51,061.17 MWh), driven primarily by its significant wind farm output (43,534.89 MWh) and contributions to heating (5289.09 MWh) and cooling (3783.83 MWh). Kalmar ranks second in total production (37,494.55 MWh), with a strong wind farm contribution (30,695.28 MWh), while heating (4778.17 MWh) and cooling (3418.28 MWh) outputs remain consistent with Stockholm. Stockholm follows closely with a total energy production of 35,101.33 MWh, primarily supported by wind farm generation (28,298.55 MWh). Sundsvall, although performing the lowest in total energy production (26,649.60 MWh), demonstrates a balanced output across heating (5316.30 MWh), cooling (3803.27 MWh), and wind farm electricity (19,084.61 MWh). These results reflect the influence of local meteorological conditions, particularly wind availability, on the hybrid system's energy performance, with Gothenburg emerging as the most productive location.

Based on the energy production results, Gothenburg, was identified as the optimal location for the proposed power plant. Fig. 23 addresses the projected CO_2 emissions, the associated emission costs, and the planned expansion of the wind farm in hectares. The results indicate that the highest CO_2 emissions (1.89 tons) and associated costs ($45.32) occur in April, corresponding to the peak energy production (9.26 MWh) and largest land use. March follows closely with 7.76 MWh production, 1.58 tons CO_2 emissions, and $37.98 in costs. Conversely, July records the lowest energy production (3.55 MWh), CO_2 emissions (0.72 tons), and costs ($17.38), reflecting reduced land use. These variations highlight the seasonal dependence of energy production on wind availability, emphasizing the need for planned expansion of the wind farm to optimize energy generation while balancing environmental impacts and land usage.

The proposed system also provides significant yearly environmental benefits to the city of Gothenburg. The system will utilize 50 ha for the wind farm and achieve an annual CO_2 reduction of 10,416.47 tons with a cost efficiency of $249,995.49 at a CO_2 emission rate of 0.20 ton/MWh. The system's total output power of 51,061.17 MWh underscores its capacity to meet energy demands sustainably while delivering substantial environmental and economic advantages to the region.

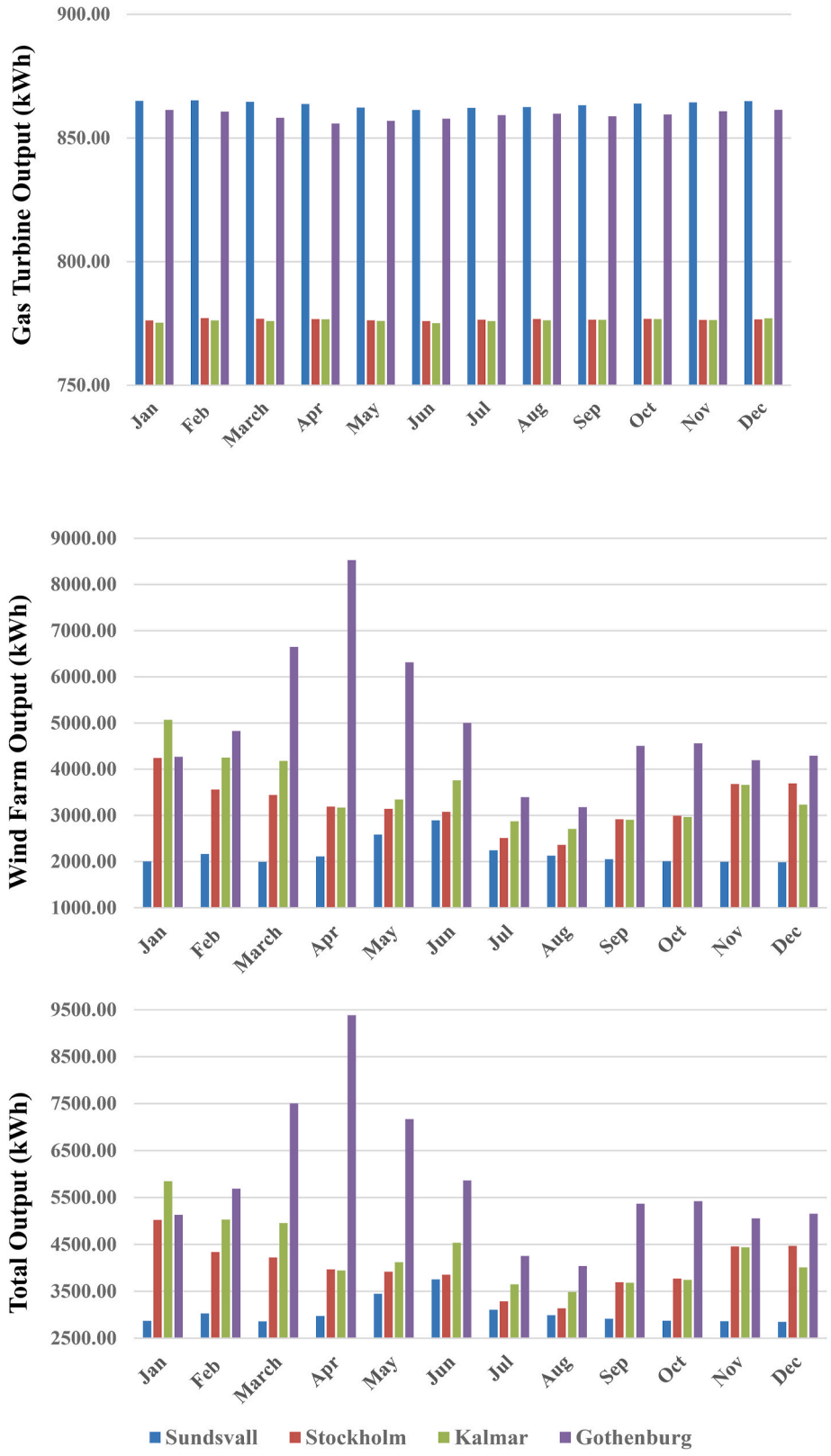

Fig. 18. Monthly changes in average net power generation relative to wind speed and temperature.

5.8. Optimal design of residential building

This section presents a simulation of a four-story residential building in Gothenburg to explore design strategies that enhance efficiency.

5.8.1. Simulation of a 4-story residential building in gothenburg using BEopt

For this study, a simulation was conducted using the BEopt program to model a four-story, sixteen-unit residential building in Gothenburg. BEopt is a tool specifically designed to identify cost-effective and energy-

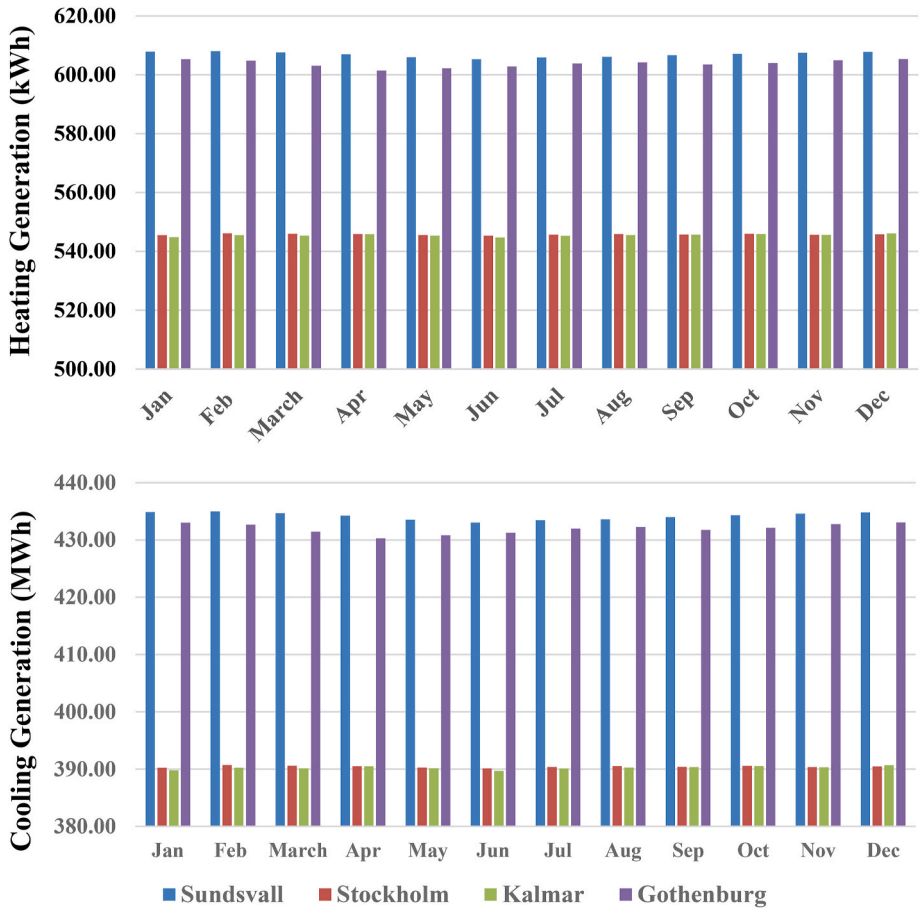

Fig. 19. Monthly changes in average heating and cooling production relative to weather conditions.

efficient designs for both new and existing homes. The key attributes of the simulated building are.

1. **16 units total** – 4 stories, each with 4 apartments, with each unit being 100 square meters in size.
2. **Two-bedroom units** with four occupants per unit and pier foundation structure.

The simulation estimated annual energy needs using BEopt to account for building characteristics. BEopt's sequential search optimization was employed to identify cost-effective efficiency measures, targeting significant whole-house energy reductions. The simulation informed energy efficiency and cost optimization for occupant comfort. The analysis aids in decision-making to optimize energy efficiency, reduce operational costs, and maintain occupant comfort.

Gothenburg's climate presents several variations reveal critical patterns influencing building performance. Fig. 24 illustrates the monthly average variations in relative humidity, solar radiation, and snow depth. The peak solar decline in winter radiation, notably in December (10.77 W/m^2), increases dependency on active heating systems, challenging energy efficiency goals. Relative humidity follows an inverse trend, peaking during winter months (January: 89.17%) and declining in spring and summer (May: 68.39%), which underscores the need for adaptive heating ventilation and air conditioning systems. The snow depth, reaching its maximum in February (20.96 cm) and notable in November (16.90 cm), can worsen thermal insulation issues and increase structural load, necessitating robust building envelope designs to maintain performance. These combined results emphasize the importance of seasonal adaptability in building design, integrating insulation, solar utilization, and ventilation strategies to address Gothenburg's climatic challenges effectively.

A detailed selection process involving various sizes and materials was conducted to develop an optimal residential building in Gothenburg, Sweden. The BEopt optimization tool was used to perform a comprehensive analysis of materials and design features to detect optimal and efficient solutions for enhancing the sustainability and performance of the building. The final choices of materials and elements are summarized in Table 6, representing the outcome of the selection process. Among the selected materials, Phase Change Materials (PCMs) stand out for their integration into the building's walls, significantly improving performance and energy efficiency. The impact of PCMs on the building's optimal outputs is as follows.

- **Thermal Regulation:** PCMs embedded within walls help regulate indoor temperatures by absorbing and releasing heat when needed. This dynamic thermal behavior reduces dependence on traditional heating and cooling approaches, contributing to a more comfortable indoor environment.
- **Energy Efficiency:** Incorporating PCMs significantly reduce energy consumption by improving the building's thermal performance. In the simulation results, the inclusion of PCMs contributed to a 10–20% reduction in annual heating and cooling energy demand compared to standard insulation materials. This energy-saving effect arises from PCMs' ability to absorb excess thermal energy during peak heating periods and release it during cooling cycles, thereby flattening temperature fluctuations and reducing heating, cooling, and ventilation system workload. This integration minimizes operational energy costs and enhances the building's compliance with ZEB targets.

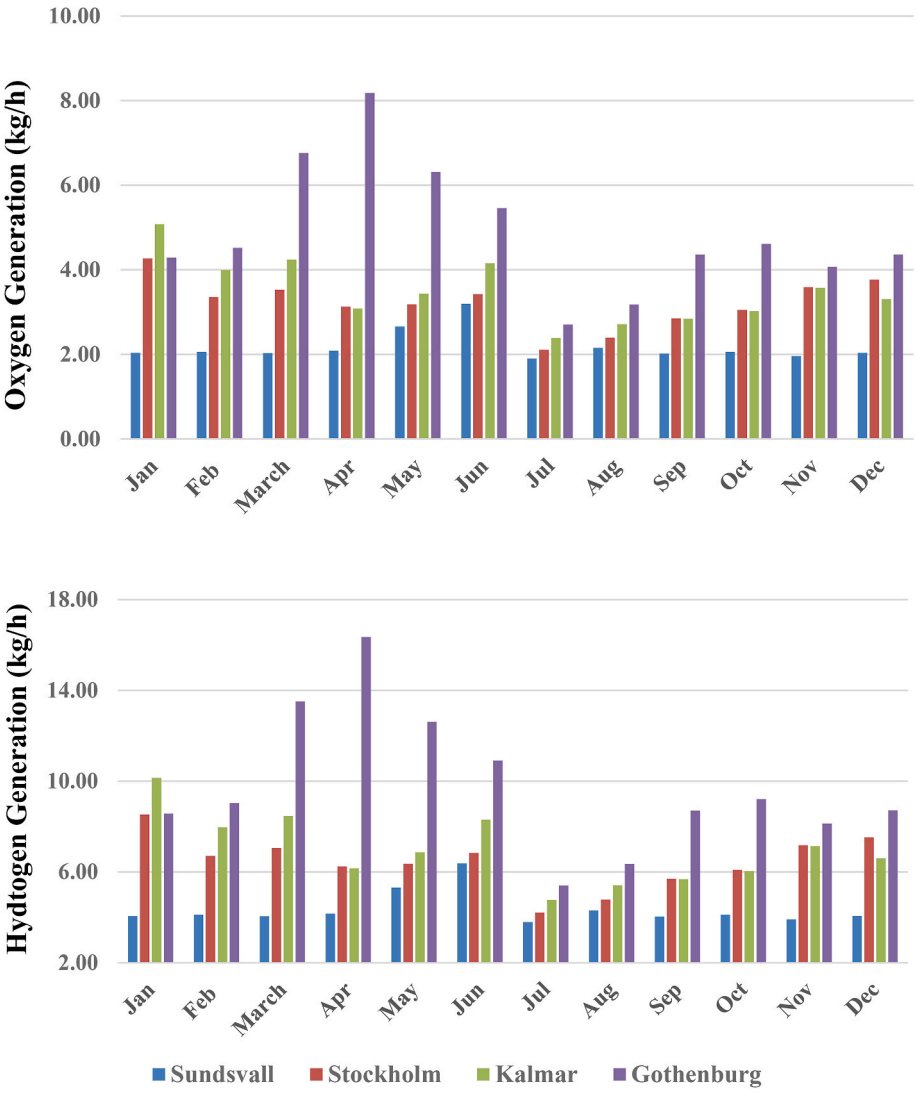

Fig. 20. Monthly changes in average oxygen and hydrogen production.

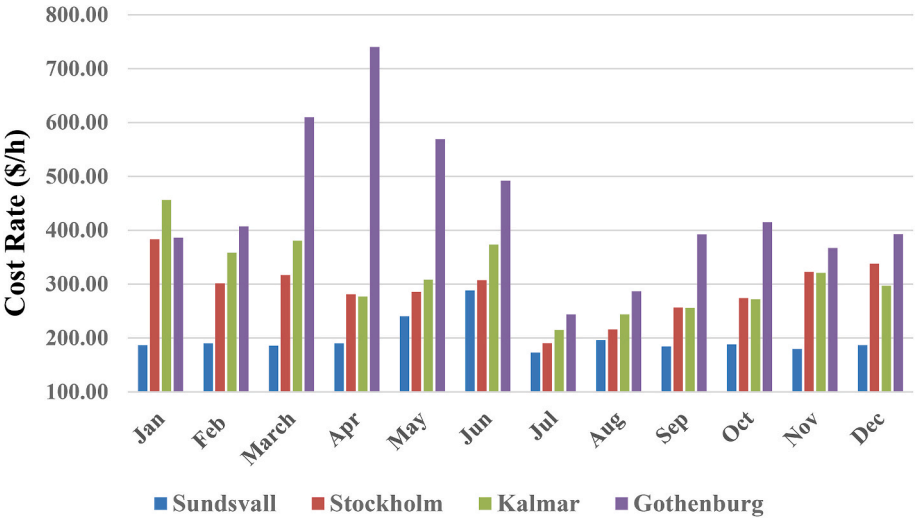

Fig. 21. Monthly changes in average cost rate with meteorological conditions.

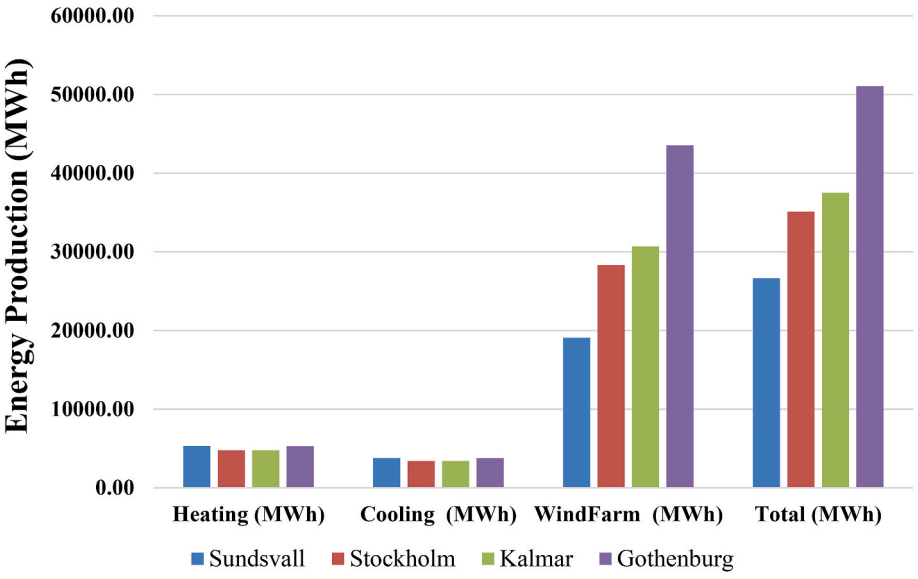

Fig. 22. Comparative analysis of energy production in the selected cities.

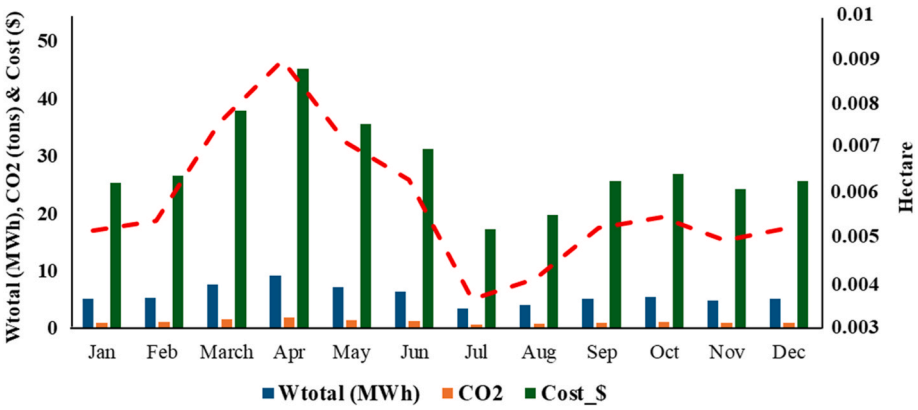

Fig. 23. CO_2 emissions, emission costs, and wind farm expansion in gothenburg.

- **Optimal Performance:** Utilizing PCMs boosts the building's thermal inertia and stability, leading to more consistent indoor temperatures and greater occupant comfort. This strategy aligns with the goal of designing an energy-efficient and sustainable structure.

The utilization of PCMs in conjunction with various wall materials exemplifies a forward-thinking approach to building design, focusing on innovation and efficiency. This strategic integration highlights the commitment to creating environmentally conscious, aesthetically appealing, and energy-efficient residential buildings.

The simulation incorporated critical thermal properties of the building envelope to ensure realistic modeling of energy consumption. The U-values of key components were as follows: walls (0.20 $W/m^2 \cdot K$), roof (0.15 $W/m^2 \cdot K$), and windows (1.10 $W/m^2 \cdot K$). These values align with regional energy efficiency standards, ensuring minimal heat loss and optimizing thermal performance. Insulation levels, such as R-20 spray foam for walls and R-38 spray foam for ceilings, were also selected to achieve these thermal properties. These parameters were integral to the building simulation, directly influencing heating and cooling demands.

Fig. 25 presents the monthly residential demand, including heating, cooling, and electricity usage in one year. Heating consumption is highest during the winter months, peaking in January (541.92 kWh), February (542.57 kWh), and December (535.48 kWh), and dropping significantly in summer, reaching its lowest in July (22.91 kWh). Cooling demand remains minimal throughout the year, with slight peaks in June (1.78 kWh), July (1.83 kWh), and August (0.99 kWh), reflecting Gothenburg's mild summer conditions. Electricity usage for lighting shows a consistent seasonal variation, with the highest demand in December (833.90 kWh) and January (795.20 kWh) due to shorter daylight hours, while the lowest occurs in June (387.57 kWh) during extended daylight periods. This figure highlights the energy production from the proposed system can significantly exceed these demands, producing a surplus of electricity, heating, and cooling energy.

Table 7 provides an analysis of the optimal cost, energy consumption, and CO_2 emissions for the buildings in Gothenburg. This Table presents the annual energy costs and Life Cycle Costs (LCC) for the studied residential building, along with energy, site energy, and CO_2 savings. The modest energy savings (0.569%) and site energy savings (0.039%) can be attributed to the cold climate of Gothenburg, where heating dominates energy demand, leaving minimal opportunities for cooling energy reductions. The building's baseline energy-efficient design and material choices also limit further energy optimization. The annual CO_2 savings (0.61%) reflect the continued reliance on grid electricity, which impacts the overall emissions reductions. To achieve greater savings, advanced strategies such as integrating high-performance insulation, renewable energy systems (e.g., solar PV and hybrid solutions), and energy storage technologies could be considered.

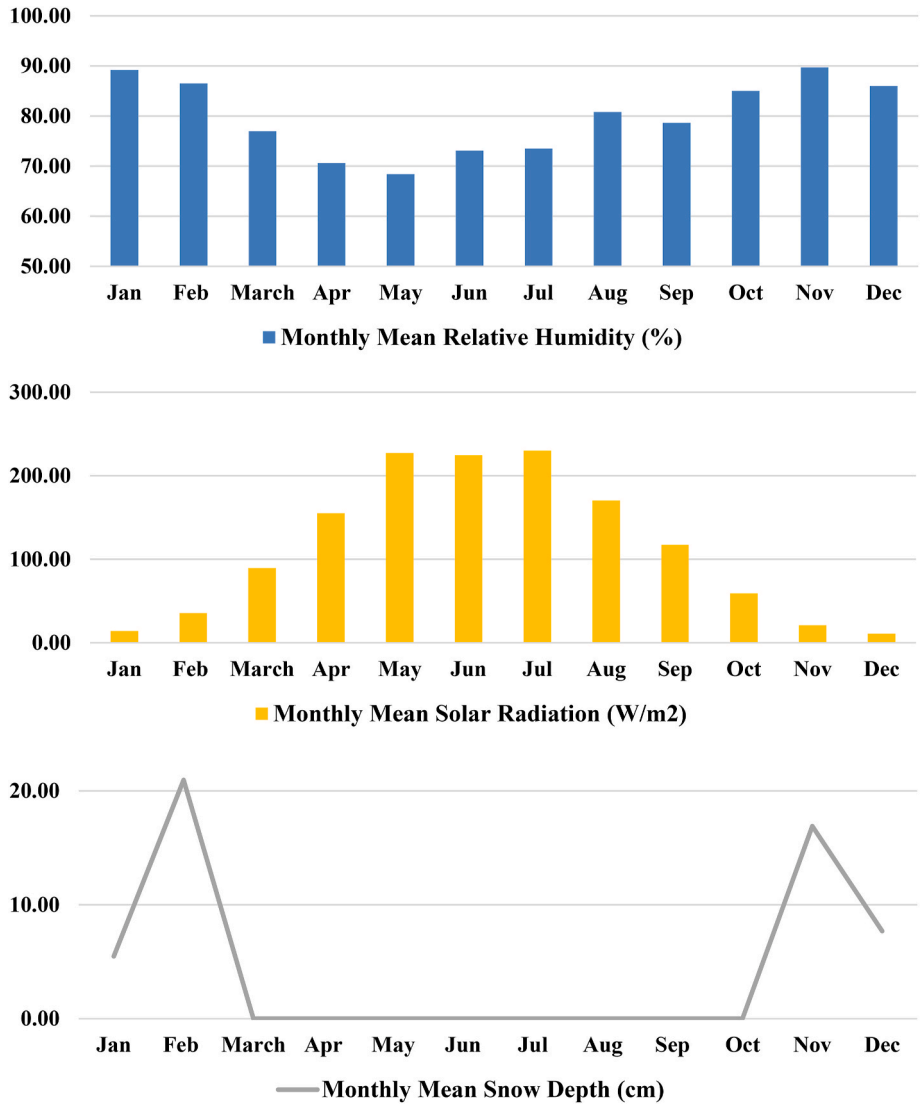

Fig. 24. Monthly average relative humidity, solar radiation, and snow depth in gothenburg.

Table 6
Optimal material selections for the residential building design in gothenburg.

Optimal Choice	Optimal Materials
Orientation	North
Wall Sheathing	OSB
Wood stud	R-20 Open cell spray foam, 2*4, 16 in o.c.
Exterior Finish	Vinyl, Light
Pier & Beam	Ceiling R-38 Opened cell spray foam
Interzonal walls	R-13 Fiberglass Batt, 2*4, 16 in o.c.
Roof material	Galvanized Steel
Finished roof	R-30+R-19 Fiberglass Batt
Carpet	80%
Floor Mass	2 in, Gypsum Concrete
Exterior wall Mass	2*5.8 in, Drywall
Windows	Low-E, Double, Non-metal, air, H-Gain
Partition wall Mass	Drywall/PCM mat
Window areas	F15 B15 L0 R0
Ceiling Mass	2*5.8 in, Drywall
Door area	30 ft^2
Eaves	2 ft
Interior Shading	Summer = 0.5, winter = 0.95
Steel stud	Uninsulated, 2*6, 24 in o.c
Doors	Fiberglass
Lighting	60% LED
Overhangs	2 ft, Frist story, Left windows
Double Wood stud	R-33 Fiberglass Batt, Gr-1, 2*4 Centered, 24 in o.c

These measures would further optimize energy efficiency, reduce costs, and enhance the building's sustainability performance across its life cycle.

Fig. 26 presents the thermal load contours for the residential building in the Swedish city, showing the daily building's energy consumption patterns for heating, cooling, and electricity over months of the year. The figure highlights the impact of different building materials on energy demand across various seasons.

Key energy distribution and consumption patterns.

- **Electricity Consumption:** The contours depict power use fluctuations influenced by building materials and environmental factors. Electricity consumption decreases significantly during winter and rises in summer.
- **Heating and Cooling Consumption:** The heating load peaks during winter, while cooling demands are highest in summer. Spring and autumn see reduced heating needs and slight increases in cooling demands.

Seasonal energy consumption patterns are.

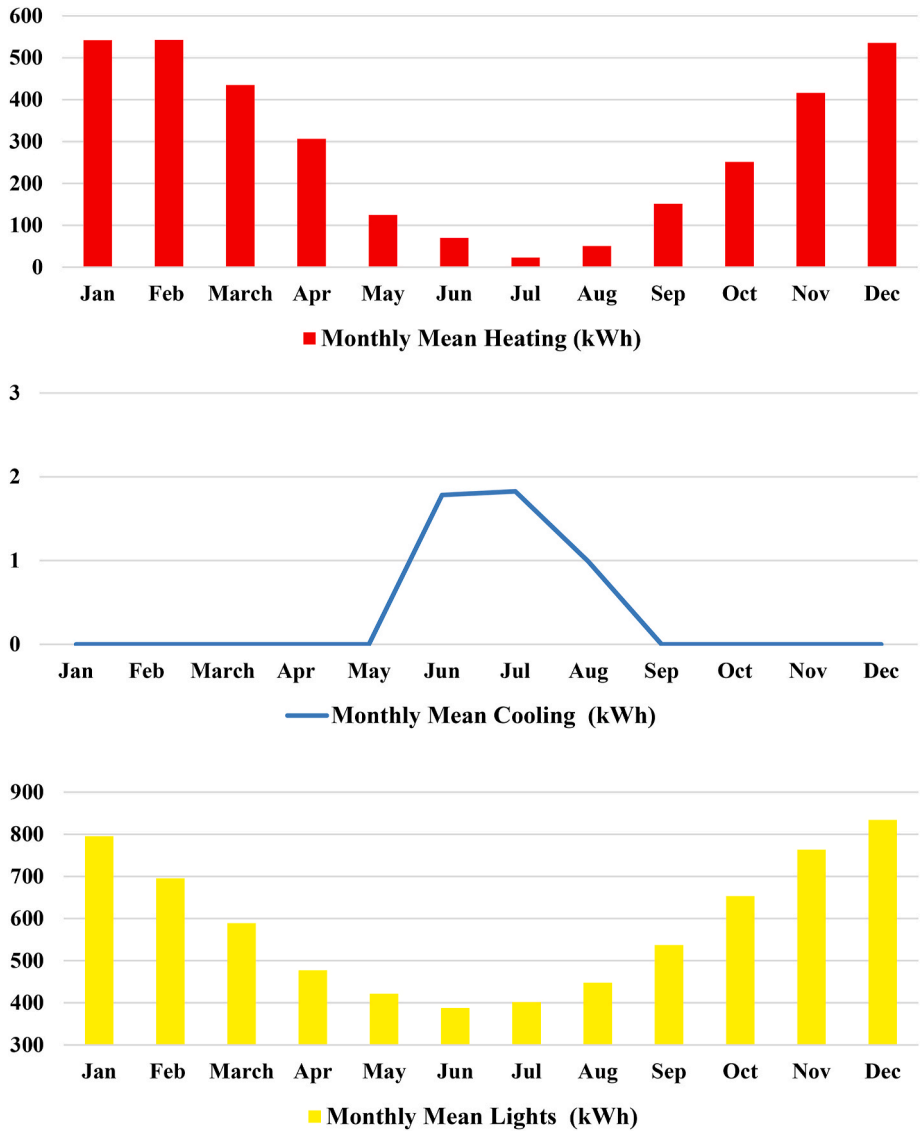

Fig. 25. Monthly heating, cooling, and electricity consumption.

Table 7
Analysis of optimal cost, energy consumption, and CO_2 emissions for residential buildings.

Parameter	Optimal Value
Annual energy costs ($/yr)	2146.909
Energy savings (%/yr)	0.569
CO_2 savings (%/yr)	0.61
CO_2 emissions (Metric tons/yr)	13.149
Energy costs, net present Value ($)	303.369
Energy costs, LCC ($)	76,963
Site energy savings (%/yr)	0.039

- **Winter:** The highest energy consumption occurs in January due to heating requirements, driven by cold temperatures and the need for insulation to maintain indoor comfort.
- **Spring and Autumn:** Heating demands decrease during these milder seasons, while cooling consumption remains low due to the temperate conditions.
- **Summer:** Cooling demands peak in July as hot temperatures increase the need for air conditioning, pushing energy consumption higher during this period.

Environmental conditions and material impact are.

- **Environmental Conditions:** The contours emphasize the influence of temperature, humidity, and solar radiation on energy consumption. These factors determine the heating and cooling demands annually.
- **Material Impact:** The figure demonstrates the impact of building materials on energy efficiency, showing how some materials offer better insulation and lower energy requirements, thus reducing the thermal load.

All things considered, Fig. 26 underscores the importance of integrating climate-responsive design and material selection to optimize energy performance and ensure sustainable, energy-efficient residential structures.

5.9. Stored energy

The evaluation of the energy performance reveals its exceptional capability to meet, and even exceed, the energy requirements of the residential building in Gothenburg, Sweden. The system generates a surplus of power, cooling, and heating energy that can be stored for

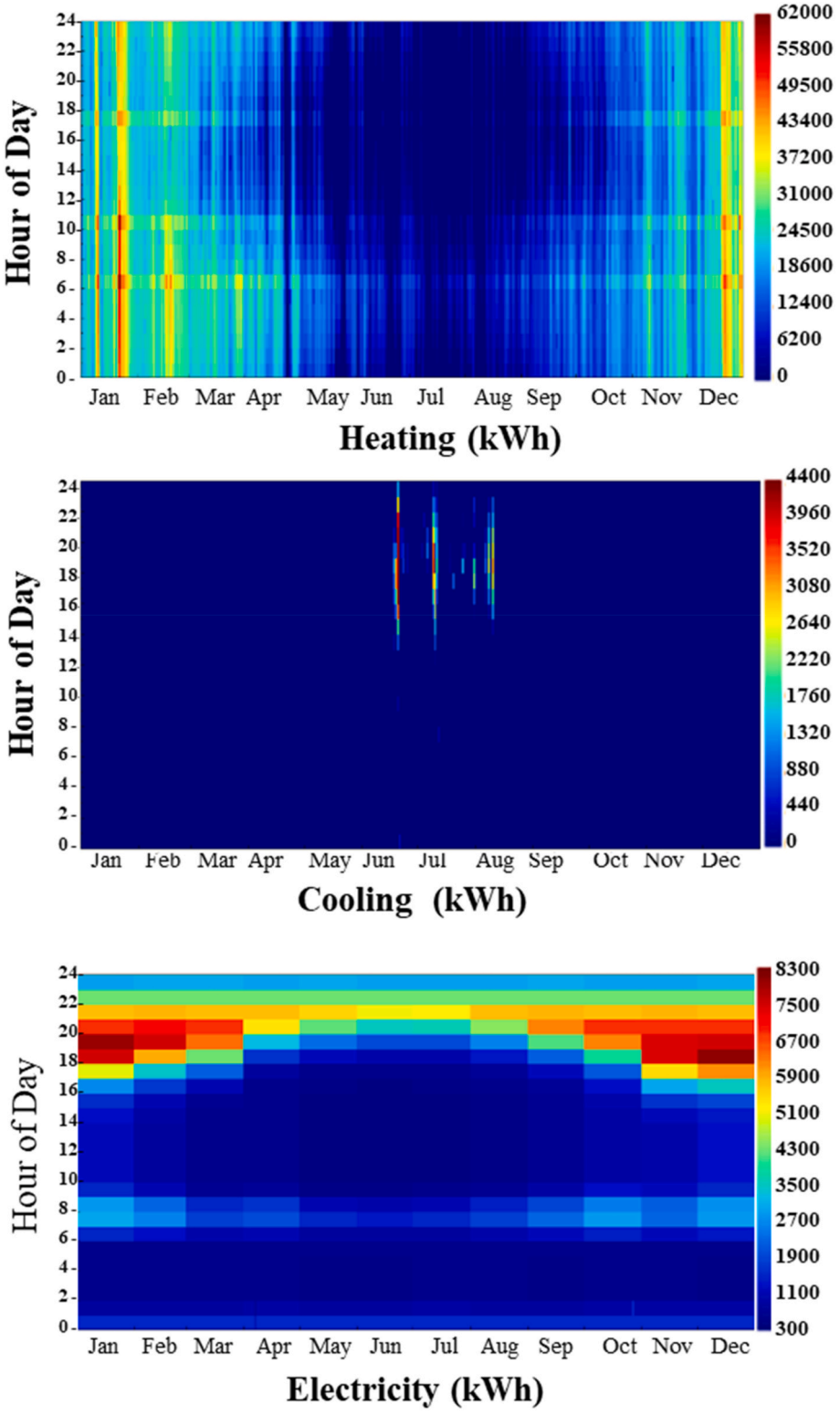

Fig. 26. Thermal load contours of the residential building in the Swedish study city.

future use, further enhancing its efficiency and potential applications.

- **Monthly Energy Storage Capabilities:** Fig. 27 illustrates the system's energy storage capabilities analyzed monthly. The figure highlights the stored cooling, heating, and electricity that can be utilized beyond the building's immediate needs.
- **Stored Cooling:** During summer months, when cooling demand is highest, the system produces excess cooling energy that can be stored. This stored cooling energy can meet future cooling demands or be applied to other processes like refrigeration or industrial applications.
- **Stored Heating:** In winter months, the system generates surplus heating energy that can be stored. This stored heating energy can

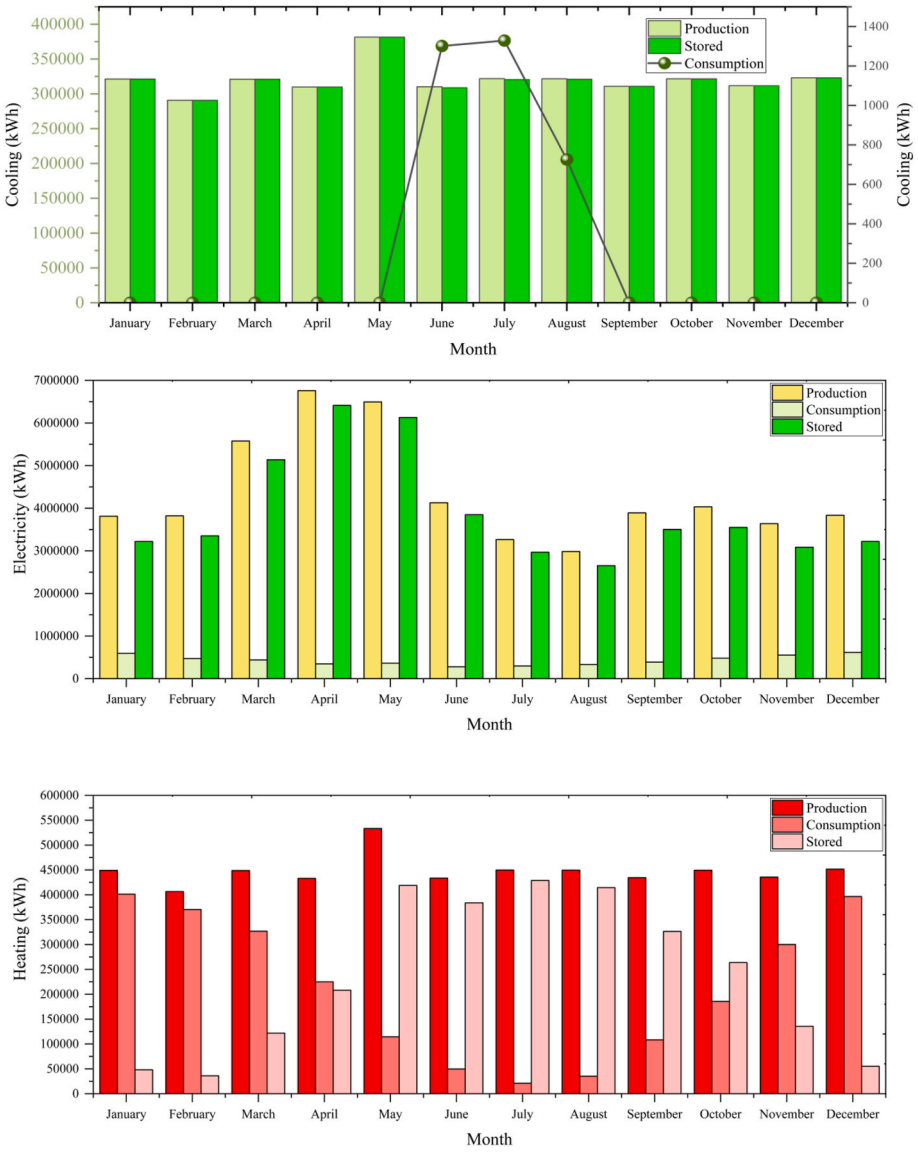

Fig. 27. Monthly energy storage.

supplement the building's heating needs during peak demand periods or be utilized for other heating purposes.

- **Stored Electricity:** The system generates surplus electricity that can be deposited for peak demand periods or fed back into the grid. This surplus electricity provides a potential revenue stream and contributes to grid stability.
- **Optimizing Energy Utilization and Cost Savings:** Storing and utilizing the surplus energy generated by the system offers multiple benefits:
  1 **Improved Energy Efficiency:** Leveraging stored energy reduces the building's reliance on external grid-supplied power, lowering operational costs and minimizing its environmental footprint
  2 **Enhanced Resilience:** Stored energy can act as a backup during grid outages or high-demand periods, ensuring uninterrupted building operations and maintaining occupant comfort
  3 **Revenue Generation:** Surplus electricity can be sold back to the grid, creating a financial return and improving the systems's economic capability
  4 **Flexibility and Adaptability:** Stored energy can be used to meet varying energy demands, allowing the building to respond to changing environmental conditions and occupancy patterns

The system's outstanding energy generation and storage capabilities can assist in transforming the residential landscape in Gothenburg, Sweden. By reducing costs, enhancing sustainability, and increasing resilience, the system provides a future-proof solution for meeting residential energy needs.

Table 8 presents the total amounts of annual stored energy. These values are calculated based on the gap between energy production and demand, highlighting the potential for repurposing surplus energy for various applications.

5.10. Scalability and modularity design

The proposed system demonstrates great potential for scaling up and integrating into larger residential complexes and commercial buildings,

Table 8
Annual energy storage of electricity, heating, and cooling in the study city.

Output Power	Consumption (kWh)	Production (kWh)	Sorted (kWh)
Cooling	3356.083	3,783,832	3,780,476
Heating	2,517,116	5,289,093	2,771,977
Electricity	5,111,372	51,061,172	45,949,800

particularly in scenarios where energy demands are higher and more varied. Its modular design not only expands by incorporating additional wind turbines but also continuously integrates other renewable sources, such as solar panels or geothermal energy, thereby adapting to the specific needs of larger buildings and ensuring adaptability. Combining hydrogen storage, with advanced and integrated solutions, such as battery-hydrogen systems, helps ensure a reliable energy supply during peak demand and effectively addresses fluctuations in renewable energy availability. This enhanced flexibility enables the system to adapt to a wide array of settings all while maintaining efficiency and resilience.

For commercial or district-level applications, the system can function as a central energy hub, producing electricity, hydrogen, and thermal energy to serve multiple buildings. By integrating intelligent energy management systems, the system can dynamically energy based on real-time demand, thereby reducing waste and optimizing performance. However, scaling the system for larger applications introduces challenges, including higher infrastructure costs, increased complexity in energy management, and substantial space requirements for renewable energy installations. Future developments may explore integrating the system into microgrids, thereby allowing energy resources to be shared among buildings, or connecting it to district heating and cooling networks to further enhance resilience. Advanced control systems, including AI-driven optimization and predictive analytics, remain critical for managing energy flows and ensuring the system maintains efficiency as it scales to larger or more complex applications. These combined advancements, coupled with support for smart grid technologies, can enable the system to scale beyond individual buildings and encompass entire neighborhoods, making it a key player in achieving urban sustainability objectives and net-zero energy goals. Furthermore, the modular design facilitates customization to match specific energy profiles, expanding the system's suitability across diverse applications, from small-scale residential neighborhoods to large industrial complexes.

5.11. Socio-economic impacts of deploying suggested systems in residential areas

Deploying the suggested system may pose certain risks and challenges that must be addressed to ensure successful implementation. High initial investment costs for wind turbines, hydrogen production, and storage facilities may discourage adoption, particularly in low-income communities. Financing solutions such as low-interest loans, tax incentives, grants, and community ownership models can ease these burdens and distribute costs more equitably. Land use and aesthetic concerns, including visual impact, noise pollution, and property value effects, require careful planning and early stakeholder engagement. Implementing design strategies, such as low-profile turbines and strategic site selection, can help balance energy generation with community needs. Ongoing maintenance is also crucial to prevent reliability issues and cost increases. Workforce training programs and predictive maintenance technologies can ensure efficient operations, while collaboration with regulatory authorities can simplify permitting processes. Public resistance, often arising from false beliefs about safety, can be mitigated through transparent communication, emphasizing the system's environmental, economic, and health benefits.

Despite these challenges, the deployment of these systems is both feasible and beneficial. Technological advancements in wind turbines, gas turbines, and hydrogen electrolyzers have enhanced efficiency and affordability, while supportive policies and successful implementations in other regions demonstrate their viability. These systems offer significant economic returns through reduced reliance on fossil fuels, energy cost savings, and income generation from surplus energy. Their modularity and scalability make them adaptable to diverse residential settings, aligning designs with specific energy demands and spatial constraints. By fostering trust through early community engagement and leveraging proven models, the deployment of hybrid renewable energy systems can drive sustainable development and resilience in residential areas.

6. Limitations and future work

The key limitation of this study is the reliance on wind energy as its variability, influenced by seasonal and geographical factors, affects energy production and efficiency. Although gas turbines and hydrogen storage partially mitigate these challenges, incorporating other renewable sources, such as solar PV or geothermal energy, could improve system adaptability in severe climates. Managing wind intermittency, equipment degradation, and the operational complexity of multiple subsystems requires advanced forecasting techniques, robust control systems, predictive maintenance tools, and redundancy in critical components. Simplifying assumptions, such as steady-state conditions, ideal turbine performance, and negligible pressure drops, may overlook real-world inefficiencies. The spatial requirements of wind farms, such as the assumed 4–6 km^2 area for 28 turbines, also introduce potential transmission losses due to the distance between the wind farm and the point of energy use. Future studies should explicitly model these losses to provide a more accurate assessment of delivered energy efficiency.

Moreover, the long-term environmental sustainability of hydrogen-based energy systems depends on advancements in green hydrogen production, efficient storage, and lifecycle management. While green hydrogen, produced through renewable-powered electrolysis, offers potential for zero-emission solutions, current production is still dominated by grey hydrogen, which emits CO_2. Transitioning to green hydrogen is driven by declining renewable energy costs, improved electrolysis efficiency, and supportive policies [58–60]. Technological trends, such as high-efficiency solid oxide electrolyzers, advanced hydrogen storage methods, and fuel cell innovations, are improving the feasibility of hydrogen as a clean energy carrier [57]. However, energy losses during hydrogen compression, storage, and transportation remain significant challenges. Comprehensive lifecycle assessments to evaluate material extraction, production, and recycling impacts are also critical for sustainability. High initial costs can be mitigated through advancements in PEM electrolyzer efficiency, cost-effective production methods, and supportive policies. Addressing these challenges will help develop a resilient, adaptable, and economically viable renewable energy system, contributing to broader adoption and supporting the global transition to sustainable energy. The energy required for hydrogen compression to liquid form was not modeled in this study to simplify the analysis. However, this process can affect overall energy efficiency. Future research should include detailed modeling of compression energy demands, multi-stage processes, and associated losses to better assess system performance and lifecycle costs.

7. Conclusion

This study addresses the challenge of intermittent renewable energy sources by introducing an innovative multifunctional hybrid system that integrates wind power, gas turbines, and Proton Exchange Membrane electrolyzers to address the challenges of intermittent renewable energy in achieving Zero Energy Building solutions. The system generates electricity, heating, cooling, and hydrogen while optimizing energy efficiency and costs through neural network-based multi-objective optimization. The results demonstrate significant advancements over previous studies, achieving a high exergy efficiency of 36.95% and an energy efficiency of 33.69% at an operational cost of $446.04 per hour, producing approximately 51,061 MWh annually to meet and exceed residential energy demands while enabling surplus energy storage and use. The proposed system also reduces CO_2 emissions by 10,416 tons annually, highlighting its environmental benefits and scalability. A key innovation lies in the integration of PEM electrolyzers for hydrogen production, showcasing hydrogen's adaptibility as a clean energy carrier for residential systems. Hydrogen was selected as the primary

storage medium for its versatility as an energy carrier, seamless integration with renewable systems, and alignment with zero-emission goals, making it a strategic choice for long-term sustainability. Compared to conventional diesel generator-based hybrid systems, this study offers improved environmental performance, cost-effectiveness, and adaptability to varying wind resources. The use of Artificial Neural Networks for optimization further enhances the system by dynamically balancing cost and efficiency, providing a novel, intelligent solution for improving performance across diverse operating conditions.

To further strengthen this approach and broaden its applicability, future work should focus on.

1. Incorporating additional renewable sources such as solar photovoltaic or geothermal energy to enhance adaptability in diverse climates.
2. Developing advanced hydrogen storage technologies to minimize energy losses during compression, storage, and transportation.
3. Conducting comprehensive lifecycle assessments to evaluate environmental impacts and sustainability across system components.
4. Exploring Artificial Intelligence-based real-time control strategies to further improve system resilience, efficiency, and operational performance.
5. Extending the system's design to industrial applications and large-scale residential complexes to assess scalability and broader applicability.

CRediT authorship contribution statement

Saleh Mobayen: Writing – original draft, Visualization, Validation, Methodology, Investigation, Formal analysis, Data curation, Conceptualization. **Ehsanolah Assareh:** Writing – original draft, Visualization, Validation, Software, Methodology, Investigation, Formal analysis, Data curation, Conceptualization. **Nima Izadyar:** Writing – review & editing, Writing – original draft, Supervision, Project administration, Methodology, Investigation. **Elmira Jamei:** Writing – review & editing, Resources, Methodology. **Mehrdad Ahmadinejad:** Validation, Software, Resources. **Amir Ghasemi:** Visualization, Software, Methodology. **Saurabh Agarwal:** Resources, Methodology, Formal analysis, Visualization, Writing – review & editing. **Wooguil Pak:** Writing – review & editing, Supervision, Project administration.

Declaration of generative AI

During the preparation of this work, the authors used an OpenAI tool to enhance language and readability. After using the tool, the authors reviewed and edited the content as needed. They take full responsibility for the final content of the publication. The authors highlight that AI's role was to assist in refining the text and language, and not to replace any critical tasks of the authors.

Declaration of competing interest

The authors declare that they have no known competing financial interests or personal relationships that could have appeared to influence the work reported in this paper.

References

[1] Gipe P, Möllerström E. An overview of the history of wind turbine development: Part I—the early wind turbines until the 1960s. Wind Eng 2022;46(6):1973–2004.
[2] Singh MB, Jain P, Singh P. Wind energy: from Past to present technology. Wind Energy Storage and Conversion: From Basics to Utilities 2024:1–16.
[3] Hannan M, et al. Wind energy conversions, controls, and applications: a review for sustainable technologies and directions. Sustainability 2023;15(5):3986.
[4] Long Y, et al. The role of global installed wind energy in mitigating CO2 emission and temperature rising. J Clean Prod 2023;423:138778.
[5] Martinez A, Iglesias G. Global wind energy resources decline under climate change. Energy 2024;288:129765.
[6] (USEIA), U.S.E.I.A.. EIA projections indicate global energy consumption increases through 2050, outpacing efficiency gains and driving continued emissions growth. 2023.
[7] Marszal AJ, et al. Zero Energy Building–A review of definitions and calculation methodologies. Energy Build 2011;43(4):971–9.
[8] Ibrahim M, et al. Building retrofitting towards net zero energy: a review. Energy Build 2024;322:114707.
[9] Fernandez MI, et al. Review of challenges and key enablers in energy systems towards net zero target: renewables, storage, buildings, & grid technologies. Heliyon 2024; 10::e40691.
[10] Chen X, Vand B, Baldi S. Challenges and strategies for achieving high energy efficiency in building districts. Buildings 2024;14(6):1839.
[11] Wu W, Skye HM. Residential net-zero energy buildings: review and perspective. Renew Sustain Energy Rev 2021;142:110859.
[12] Aljashaami BA, et al. Recent improvements to heating, ventilation, and cooling technologies for buildings based on renewable energy to achieve zero-energy buildings: a systematic review. Results in Engineering 2024:102769.
[13] Assareh E, et al. A proposal on a co-generation system accompanied with phase change material to supply energy demand of a hospital to make it a zero energy building (ZEB). Energy Build 2024;318:114478.
[14] Hawks M, Cho S. Review and analysis of current solutions and trends for zero energy building (ZEB) thermal systems. Renew Sustain Energy Rev 2024;189:114028.
[15] Pawar R, et al. Renewable energy hybridization: a comprehensive review of integration strategies for efficient and sustainable power generation. Clean Technol Environ Policy 2024:1–18.
[16] Karlsson A, Holm D. Common barriers and challenges in current nZEB practice in Europe. IVL svenska miljöinstitutet. 2014.
[17] Di Turi S, Ronchetti L, Sannino R. Towards the objective of Net ZEB: detailed energy analysis and cost assessment for new office buildings in Italy. Energy Build 2023;279:112707.
[18] Jamal T, Salehin S. Hybrid renewable energy sources power systems. In: Hybrid renewable energy systems and microgrids. Elsevier; 2021. p. 179–214.
[19] Zhou H, et al. Hydrogen-fueled gas turbines in future energy system. Int J Hydrogen Energy 2024;64:569–82.
[20] Guduru R, et al. Hydrogen as an energy carrier. In: Subsurface hydrogen energy storage. Elsevier; 2025. p. 31–61.
[21] Cheekatamarla P. Hydrogen and the global energy transition—path to sustainability and adoption across all economic sectors. Energies 2024;17(4):807.
[22] Kamran M, Turzyński M. Exploring hydrogen energy systems: a comprehensive review of technologies, applications, prevailing trends, and associated challenges. J Energy Storage 2024;96:112601.
[23] Le TT, et al. Fueling the future: a comprehensive review of hydrogen energy systems and their challenges. Int J Hydrogen Energy 2024;54:791–816.
[24] Molière M. The fuel flexibility of gas turbines: a review and retrospective outlook. Energies 2023;16(9):3962.
[25] Morales MJM, Blondeau J, De Paepe W. Assessing the impact of CH4/H2 blends on the thermodynamic performance of aero-derivative gas turbine CHP configurations. Int J Hydrogen Energy 2024;67:159–71.
[26] Yu S, et al. Hydrogen-based combined heat and power systems: a review of technologies and challenges. Int J Hydrogen Energy 2023;48(89):34906–29.
[27] Granet I, Alvarado J, Bluestein M. Thermodynamics and heat power. CRC Press; 2020.
[28] Temiz M, Dincer I. Enhancement of solar energy use by an integrated system for five useful outputs: system assessment. Sustain Energy Technol Assessments 2021;43:100952.
[29] Chen Y, et al. Exergy-economic analysis and multi-objective optimization of a multi-generation system based on efficient waste heat recovery of combined wind turbine and compressed CO2 energy storage system. Sustain Cities Soc 2023;96:104714.
[30] Nnabuife SG, et al. Integration of renewable energy sources in tandem with electrolysis: a technology review for green hydrogen production. Int J Hydrogen Energy 2024. https://doi.org/10.1016/j.ijhydene.2024.06.342.
[31] Akyüz ES, Telli E, Farsak M. Hydrogen generation electrolyzers: paving the way for sustainable energy. Int J Hydrogen Energy 2024;81:1338–62.
[32] Bodkhe RG, et al. A review of renewable hydrogen generation and proton exchange membrane fuel cell technology for sustainable energy development. Int J Electrochem Sci 2023;18(5):100108.
[33] Sikiru S, et al. Hydrogen-powered horizons: transformative technologies in clean energy generation, distribution, and storage for sustainable innovation. Int J Hydrogen Energy 2024;56:1152–82.
[34] Zhao X, et al. Optimization and analysis of an integrated energy system based on wind power utilization and on-site hydrogen refueling station. Int J Hydrogen Energy 2023;48(57):21531–43.
[35] Canale L, et al. An overview on functional integration of hybrid renewable energy systems in multi-energy buildings. Energies 2021;14(4):1078.
[36] Thirunavukkarasu M, Sawle Y, Lala H. A comprehensive review on optimization of hybrid renewable energy systems using various optimization techniques. Renew Sustain Energy Rev 2023;176:113192.
[37] Khan T, Yu M, Waseem M. Review on recent optimization strategies for hybrid renewable energy system with hydrogen technologies: state of the art, trends and future directions. Int J Hydrogen Energy 2022;47(60):25155–201.
[38] Mayer MJ, Szilágyi A, Gróf G. Environmental and economic multi-objective optimization of a household level hybrid renewable energy system by genetic algorithm. Appl Energy 2020;269:115058.

[39] Mousavi S, et al. Data-driven prediction and optimization toward net-zero and positive-energy buildings: a systematic review. Build Environ 2023;242:110578.
[40] Yan B, Hao F, Meng X. When artificial intelligence meets building energy efficiency, a review focusing on zero energy building. Artif Intell Rev 2021;54(3): 2193–220.
[41] Zupan J. Introduction to artificial neural network (ANN) methods: what they are and how to use them. Acta Chim Slov 1994;41(3):327.
[42] Mehrpooya M, et al. Investigation of a hybrid solar thermochemical water-splitting hydrogen production cycle and coal-fueled molten carbonate fuel cell power plant. Sustain Energy Technol Assessments 2021;47:101458.
[43] Razmi AR, Janbaz M. Exergoeconomic assessment with reliability consideration of a green cogeneration system based on compressed air energy storage (CAES). Energy Convers Manag 2020;204:112320.
[44] Alpegiani F, et al. Ultra high efficient power generation with SOFC-gas turbine systems: different options for 80%+ efficiency power cycles. In: Turbo expo: power for land, sea, and air. American Society of Mechanical Engineers; 2023.
[45] Dincer I, Rosen MA, Ahmadi P. Optimization of energy systems. John Wiley & Sons; 2017.
[46] Delpisheh M, et al. Desalinated water and hydrogen generation from seawater via a desalination unit and a low temperature electrolysis using a novel solar-based setup. Int J Hydrogen Energy 2021;46(10):7211–29.
[47] Bejan A, Tsatsaronis G, Moran MJ. Thermal design and optimization. John Wiley & Sons; 1995.
[48] Shakibi H, et al. Exergoeconomic and optimization study of a solar and wind-driven plant employing machine learning approaches; a case study of Las Vegas city. J Clean Prod 2023;385:135529.
[49] Ioroi T, et al. Thin film electrocatalyst layer for unitized regenerative polymer electrolyte fuel cells. J Power Sources 2002;112(2):583–7.
[50] Li S, et al. Intelligent optimization of eco-friendly H2/freshwater production and CO2 reduction layout integrating GT/rankine cycle/absorption chiller/TEG unit/PEM electrolyzer/RO section. Process Saf Environ Protect 2024; 189: p.204-218.
[51] Sharifishourabi M, Dincer I, Mohany A. Performance and environmental impact evaluations of a novel multigeneration system with sonic hydrogen production and energy storage options. J Energy Storage 2024;78:109987.
[52] Sami S, Gholizadeh M, Deymi-Dashtebayaz M. An applicable multi-generation system for different climates from energy, exergy, exergoeconomic, economic, and environmental (5E) perspectives. Sustain Cities Soc 2024;100:105057.
[53] Nikitin A, et al. Energy, exergy, economic and environmental (4E) analysis using a renewable multi-generation system in a near-zero energy building with hot water and hydrogen storage systems. J Energy Storage 2023;62:106794.
[54] Cai S, et al. Flexible load regulation method for a residential energy supply system based on proton exchange membrane fuel cell. Energy Convers Manag 2022;258: 115527.
[55] Ozlu S, Dincer I. Performance assessment of a new solar energy-based multigeneration system. Energy 2016;112:164–78.
[56] Baseer M, Alqahtani A, Rehman S. Techno-economic design and evaluation of hybrid energy systems for residential communities: case study of Jubail industrial city. J Clean Prod 2019;237:117806.
[57] Łosiewicz B. Technology for green hydrogen production: desk analysis. Energies 2024;17(17):4514.
[58] Gado MG. Techno-economic-environmental assessment of green hydrogen production for selected countries in the Middle East. Int J Hydrogen Energy 2024; 92:984–99.
[59] Hammi Z, et al. Green hydrogen: a holistic review covering life cycle assessment, environmental impacts, and color analysis. Int J Hydrogen Energy 2024;80: 1030–45.
[60] Wang Y, et al. In-situ green hydrogen production from offshore wind farms, a prospective review. Renew Energy 2024:122099.